Pyrazolates advance cerium chemistry: a Ce^{III}/Ce^{IV} redox equilibrium with benzoquinone

Daniel Werner, Glen B. Deacon, Peter C. Junk and Reiner Anwander*

Supporting information

Spectra and crystal structures S3

Spectra and crystal structures

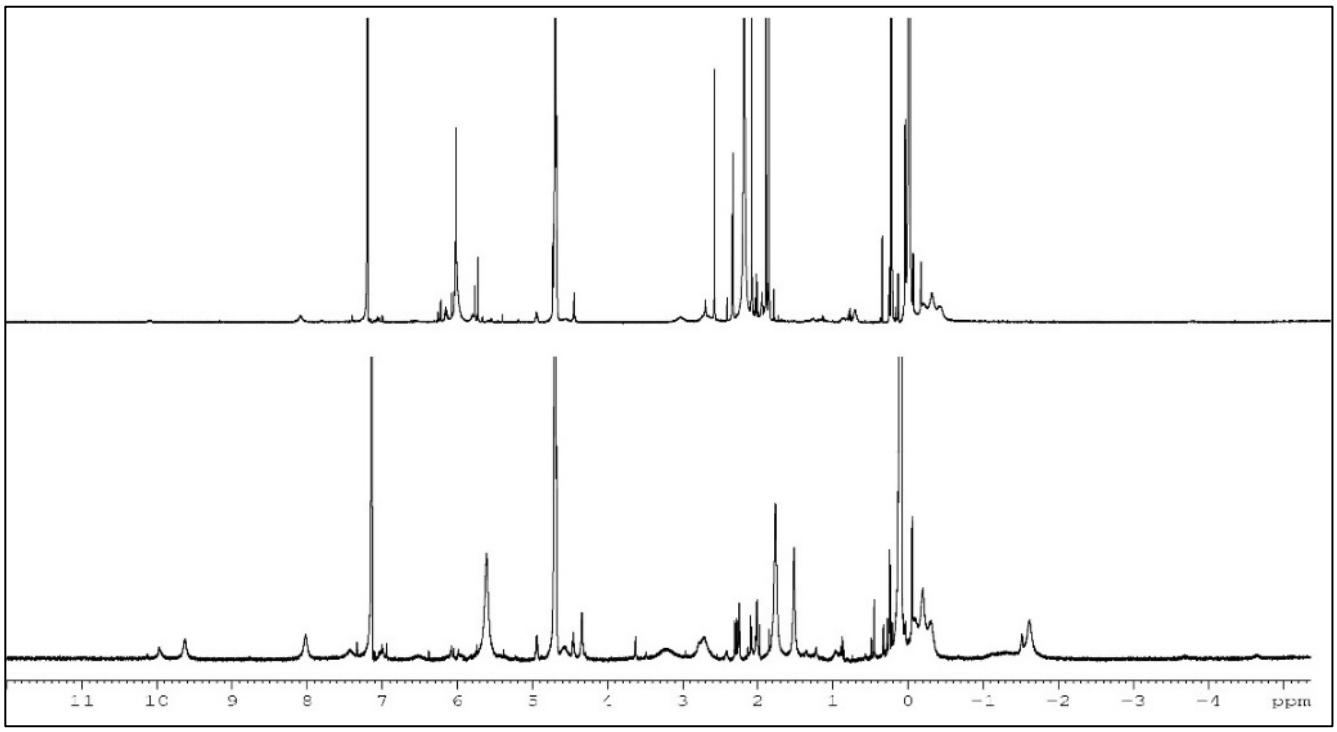

Figure S1. ^{1}H NMR (400 MHz) spectra of the protonolysis reaction mixture from $Ce[N(SiHMe_2)_2]_4$ and Me_2pzH in C_6D_6 at 300 K (*top,* after 5-10 minutes; *bottom*, after two days).

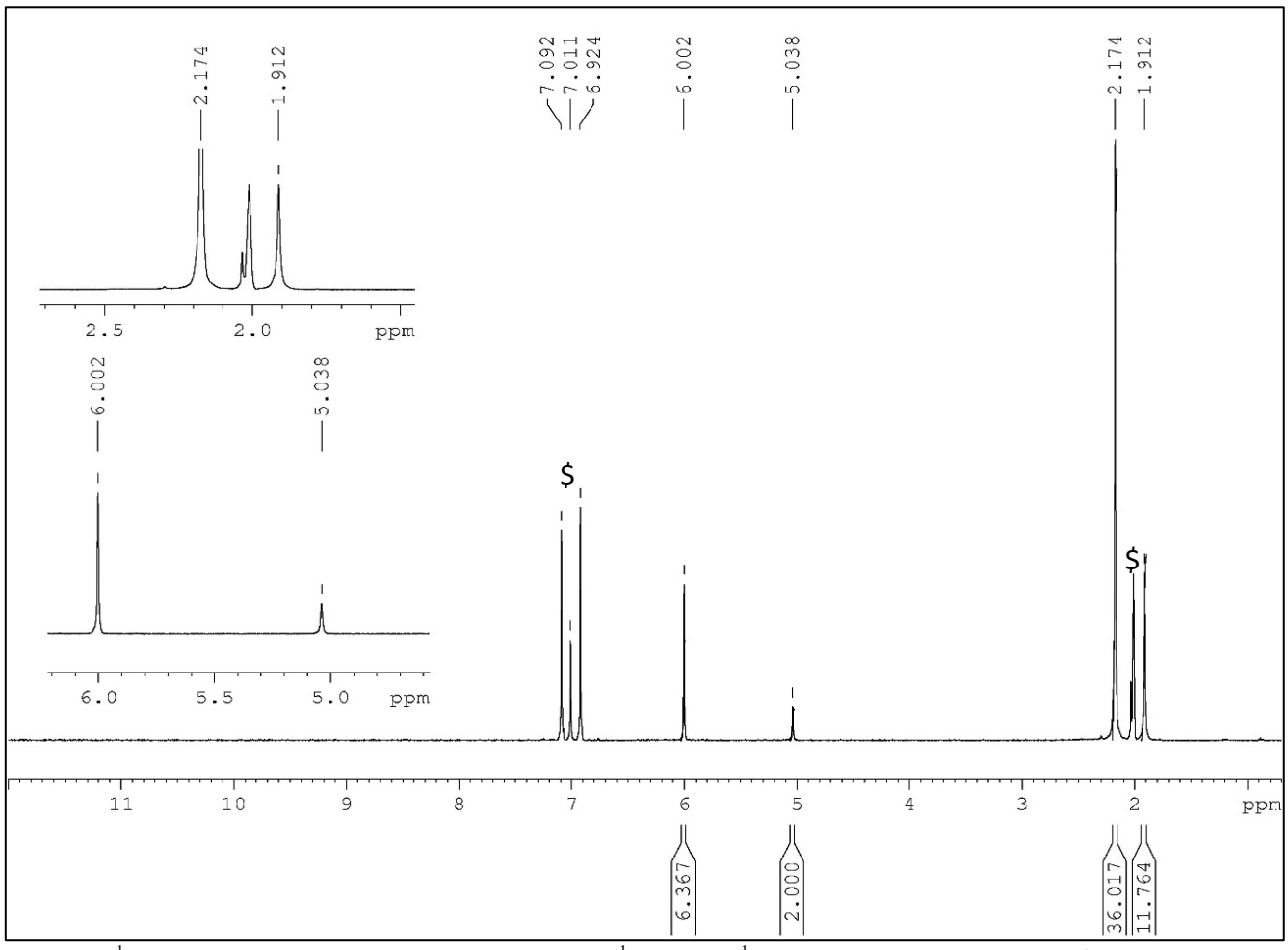

Figure S2. ^{1}H NMR (500 MHz) spectrum of $[Ce(Me_2pz)_4]_2 \cdot {}^1/_4PhMe$ (**2**$\cdot {}^1/_4$PhMe) in toluene-d_8 at 193 K ($ = toluene-d_8).

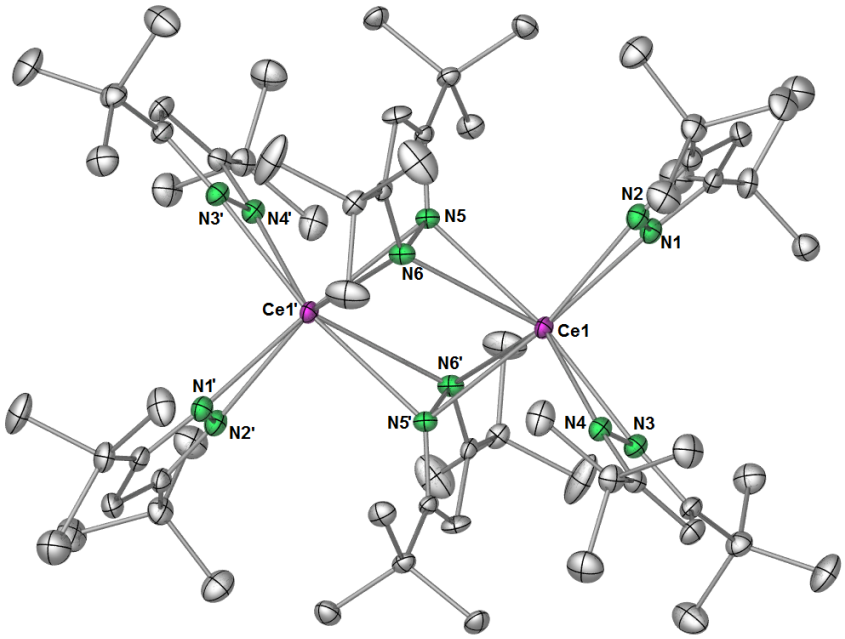

Figure S3. Molecular structure of [Ce(*t*Bu$_2$pz)$_3$]$_2$ (**3**). Ellipsoids are shown at 50% probability and hydrogen atoms have been removed for clarity. Selected bond lengths (Å): Ce1-N1 2.431(2), Ce1-N2 2.415(2), Ce1-N3 2.426(2), Ce1-N4 2.425(2), Ce1-N5 2.577(2), Ce1-N6 2.735(2), Ce1-N5′ 2.590(2), Ce1-N6′ 2.757(2).

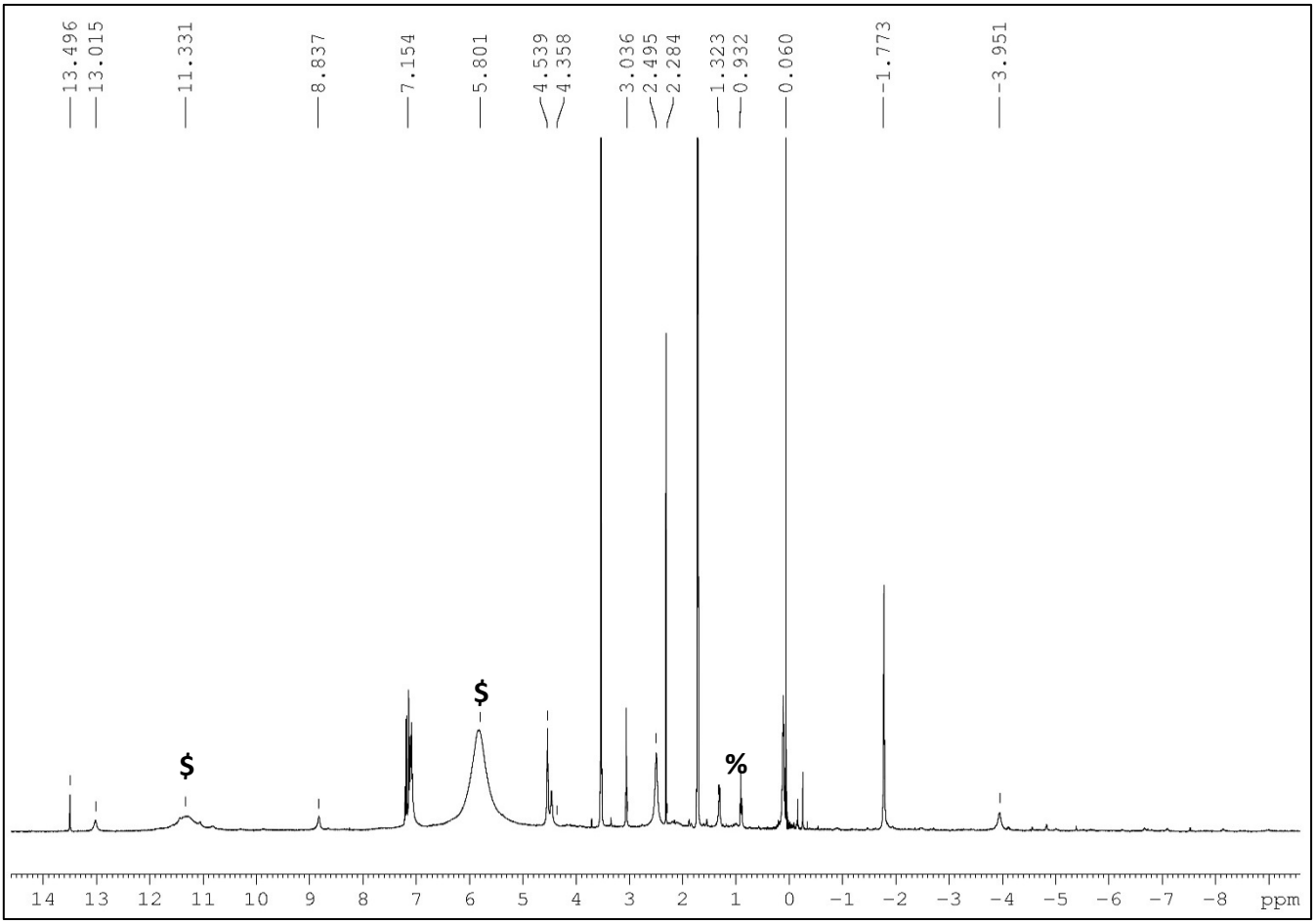

Figure S4. ^{1}H NMR (400 MHz) spectrum of the reaction of [Ce(Me$_2$pz)$_3$] (**1**) with bq in THF-d$_8$ at 300 K (crystallization from this reaction mixture gave [Ce$_3$(Me$_2$pz)$_5$(pchd)$_2$(thf-d$_8$)$_2$]·1^1/$_2$THF-d$_8$, (**3a**·1^1/$_2$THF-d$_8$). Due to ligand scrambling no meaningful assignments could be given ($ = "[Ce(Me$_2$pz)$_3$]", % = trace *n*-hexane impurity).

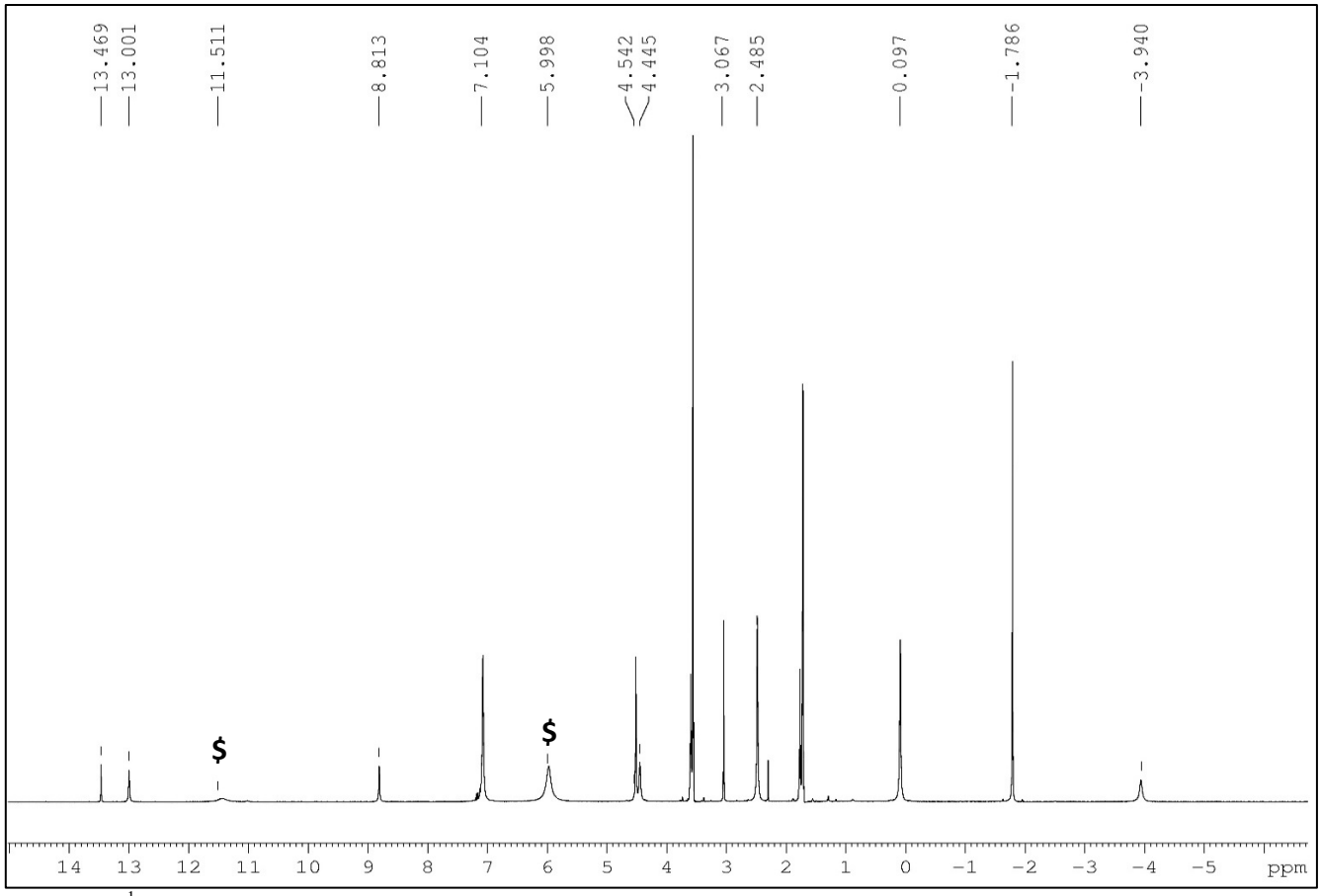

Figure S5. ^{1}H NMR (400 MHz) spectrum of isolated [$Ce_3(Me_2pz)_5(pchd)_2(thf)$] (**5a**–thf) in THF-$d_8$ at 300 K. No meaningful assignments could be made, however as "[$Ce(Me_2pz)_3$]" was identified ($) it is apparent that some degree of ligand scrambling occured.

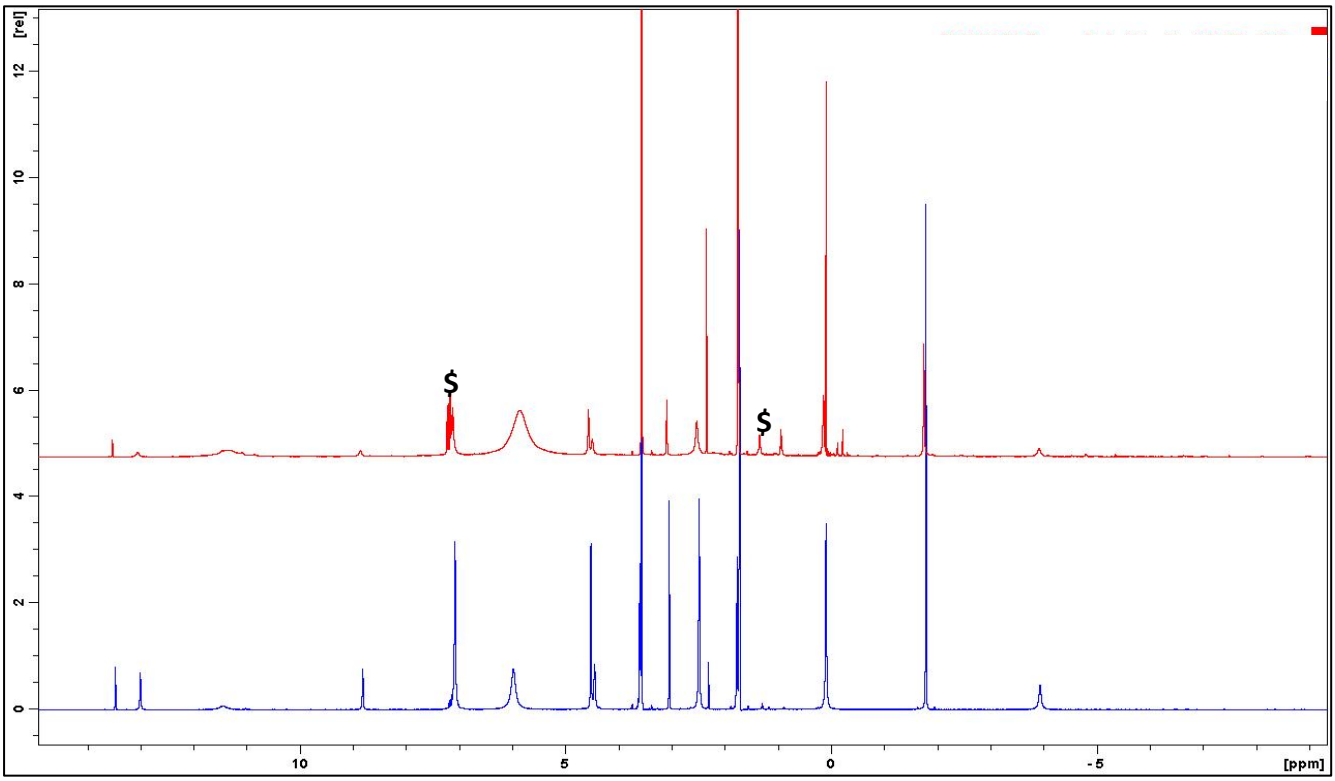

Figure S6. Overlapping spectra of isolated [$Ce_3(Me_2pz)_5(pchd)_2(thf)$] (**5a**-thf, bottom, see Figure S5), and the reaction between "[$Ce(Me_2pz)_3$]" and half an equivalent of bq (top, see Figure S4). This highlights the selectivity of the reaction showing **5a** is the predominant product ($ - trace solvent impurity).

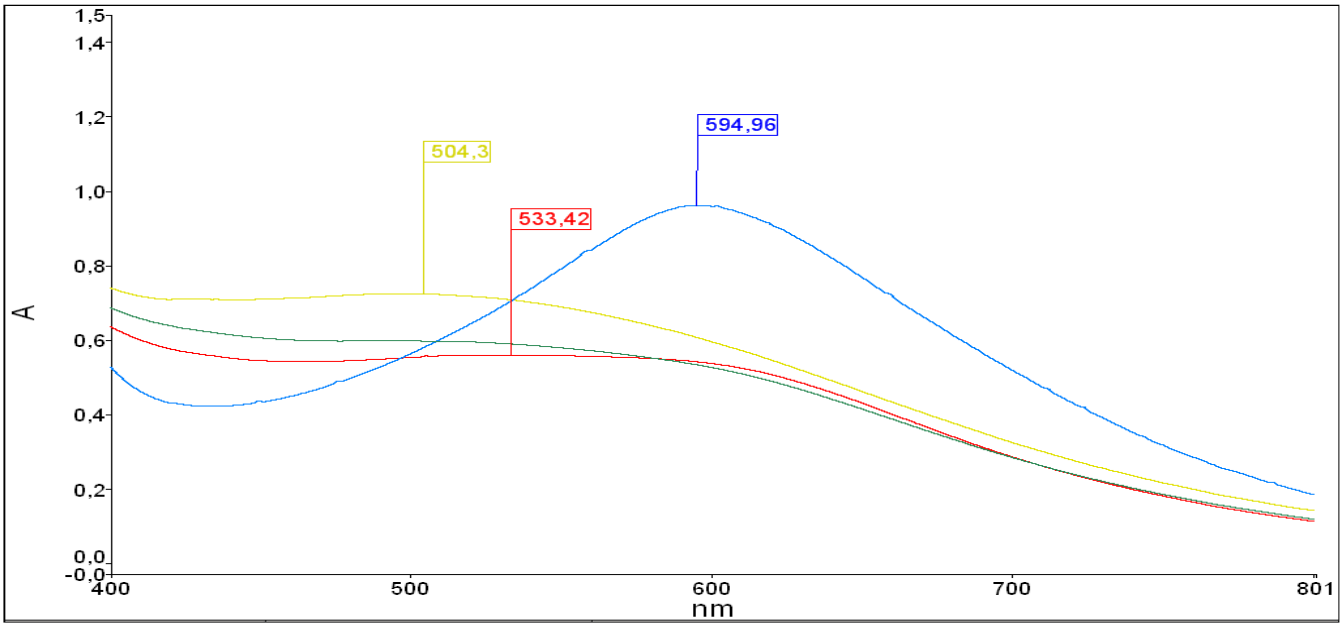

Figure S7. UV-vis spectra of the reaction between **1(thf)** and a slight excess of bq in THF. Blue line: at -95 °C; red line at -15 °C; green line at + 5 °C, yellow line at 25 °C.

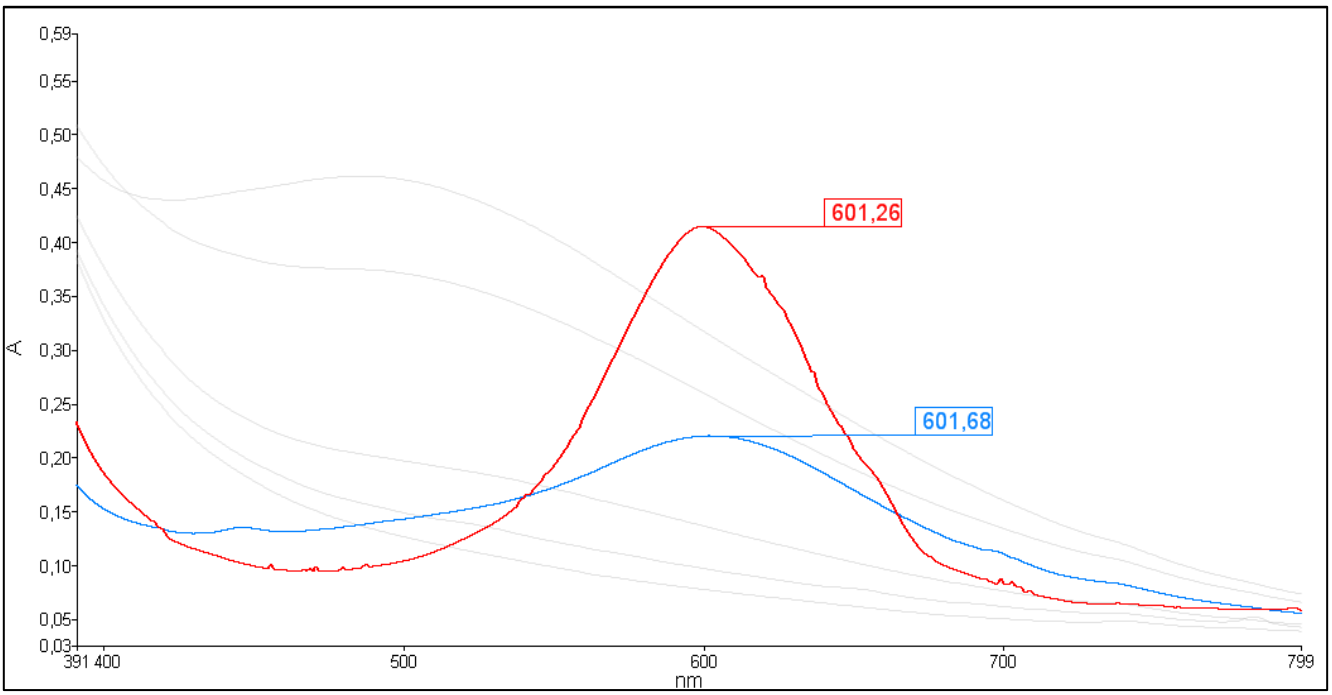

Figure S8. UV-vis spectra of the reaction between **1(thf)** and bq (with a slight excess of **1(thf)**) in THF. Red: at -95 °C on addition; blue: at -95 °C after ~1 h.

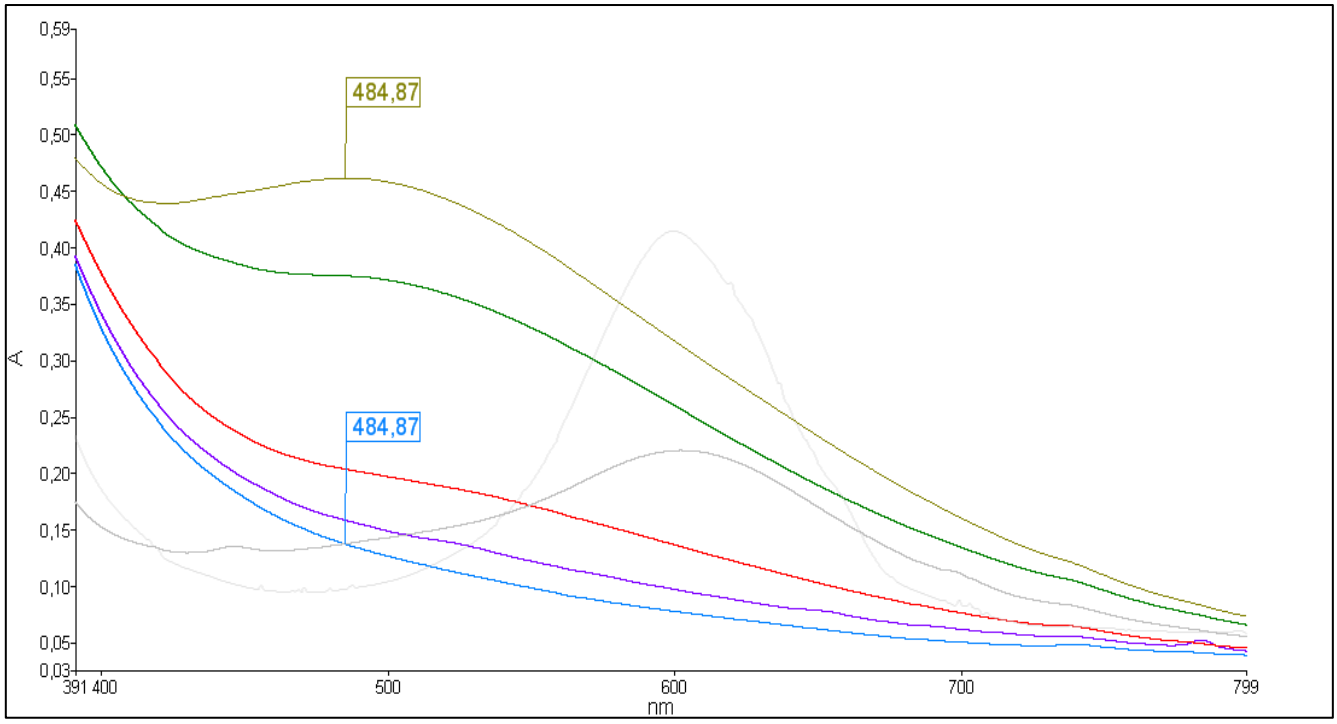

Figure S9. UV-vis spectra of the reaction between **1(thf)** and bq (with a slight excess of **1(thf)**) in THF. Dark yellow: at -30 °C after one min; dark green: at 5 °C after one min; red: at 30 °C after one min; purple: at 30 °C after 20 min; blue: at 60 °C after one min.

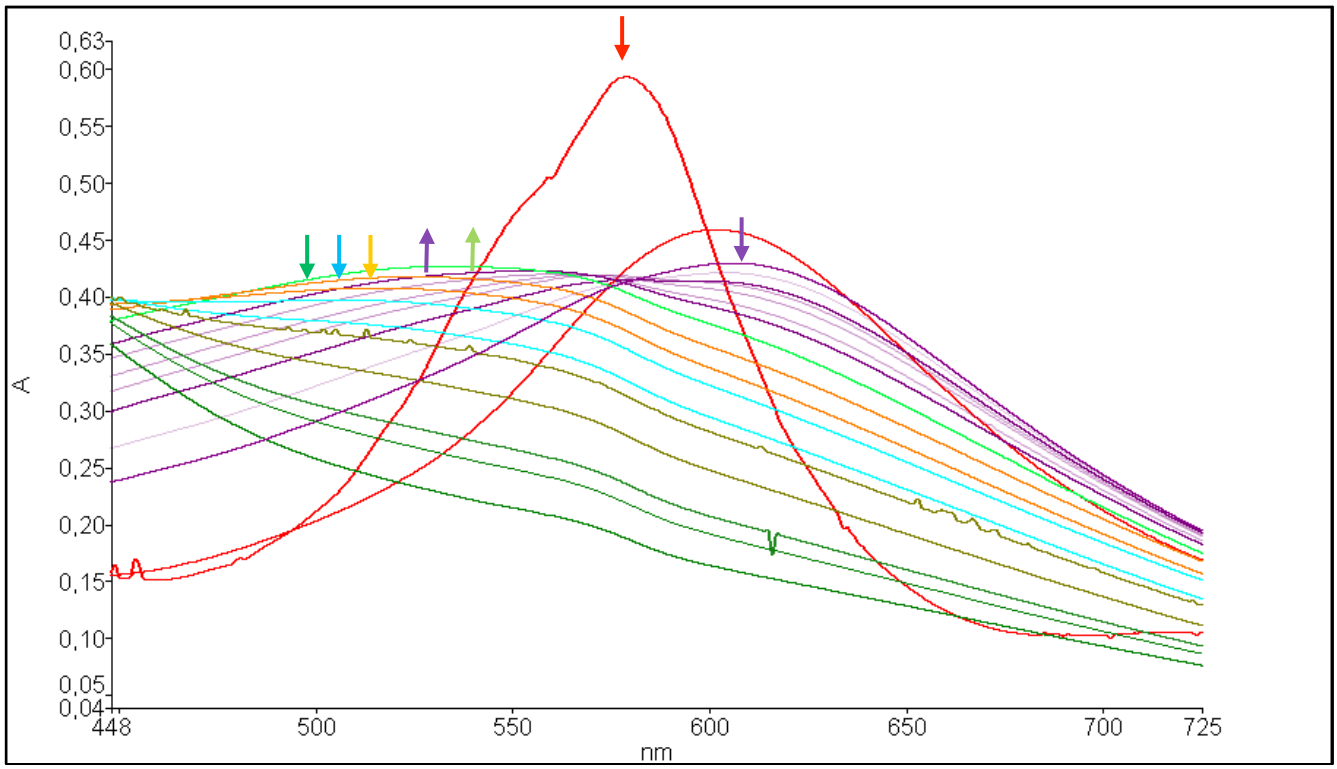

Figure S10. Compiled UV-vis spectra for the reaction between **1(thf)** (in slight excess) and bq, in THF monitored at varied temperatures. Red lines: at -95 °C after bq addition and after 1 h; purple lines: at -50 °C after 1 min and two h (including 45 min at -70 °C); light green lines: at -40 °C after one h; yellow lines: -25 °C after 1 min and half an h; olive green lines: at -5 °C after one min and half an h; emerald green lines: at +10 °C after one, 5, and 15 min, respectively.

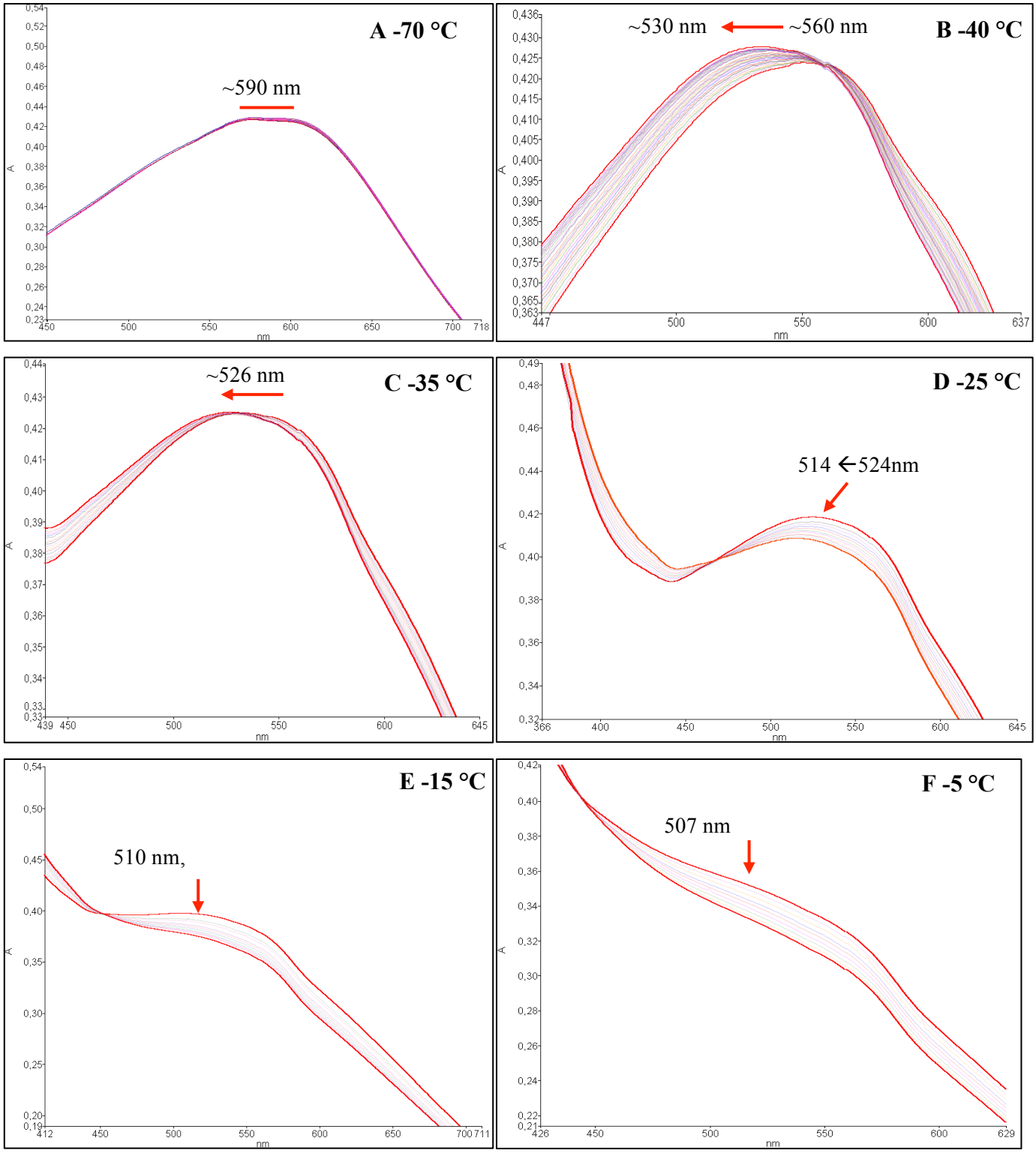

Figure S11. Compiled UV-vis spectra for the slow cooling of a mixture of **1(thf)** and bq; highlighted lines show the start and end of the cooling process at each temperatures. **A**: at -70 °C (for 45 min) analyzed after standing at -50 °C for 18 min. **B**: at -40 °C for 1 min and 1 h. **C**: at -35 °C for 1 min and 45 min. **D**: at ~-25 °C for 1 min and 30 min (ΔAbs: 0.01). **E**: at -15 °C for 1 min and half an h (ΔAbs: 0.03). **F**: at -15 °C for 1 min and half an h (ΔAbs: 0.03).

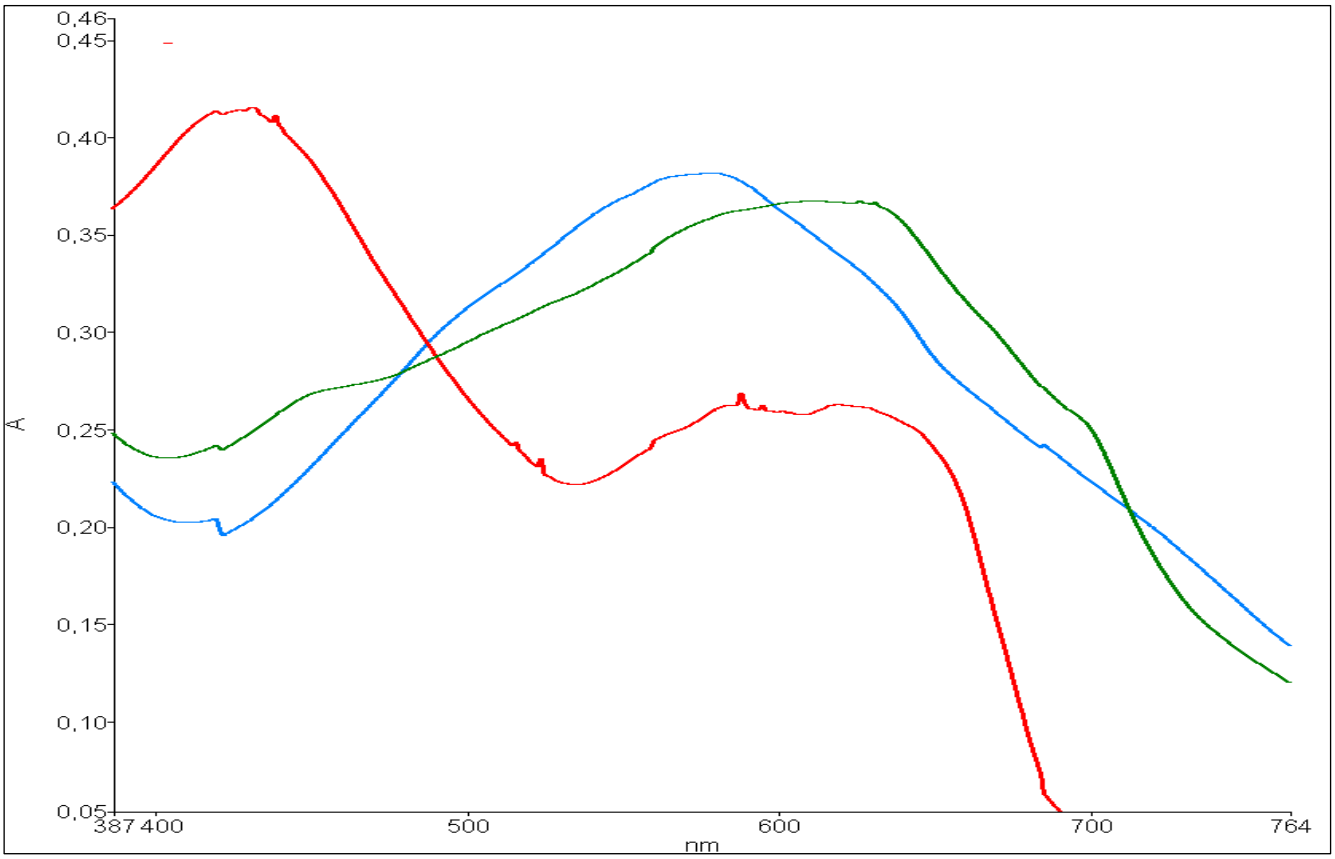

Figure S12. UV-vis spectra of the reaction between **2** and H_2hq in THF at -95 °C. Red line: immediately after addition; green line: after 4 min; blue line: after 8 min (concentration of injected H_2hq: 0.0069 M^{-1} L^{-1}).

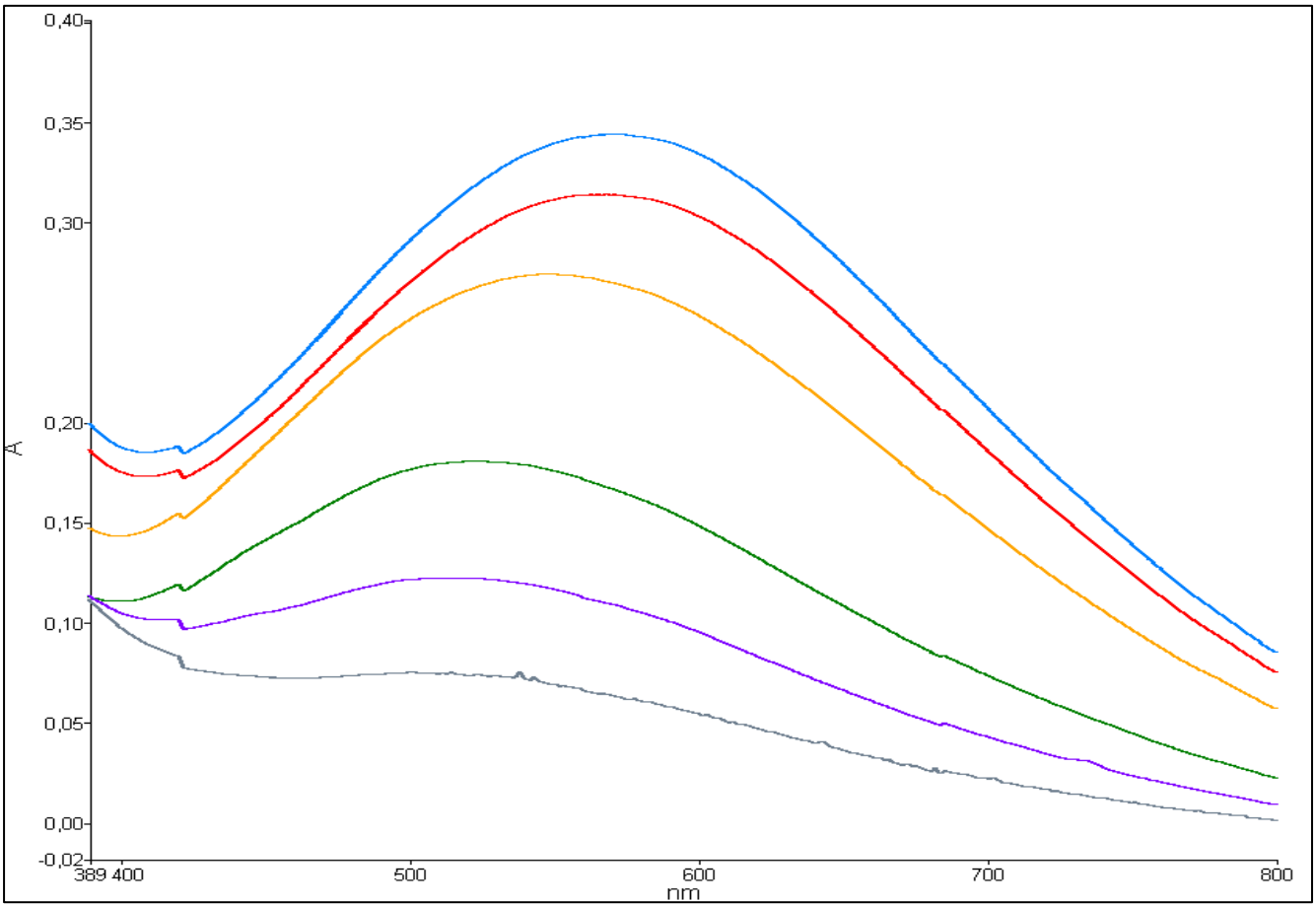

Figure S13. UV-vis spectra of the reaction between **2** and H_2hq in THF at -75 °C (blue line), -55 °C (red line), -35 °C (yellow line), 5 °C (green line), 15 °C (purple line), 25 °C (grey line).

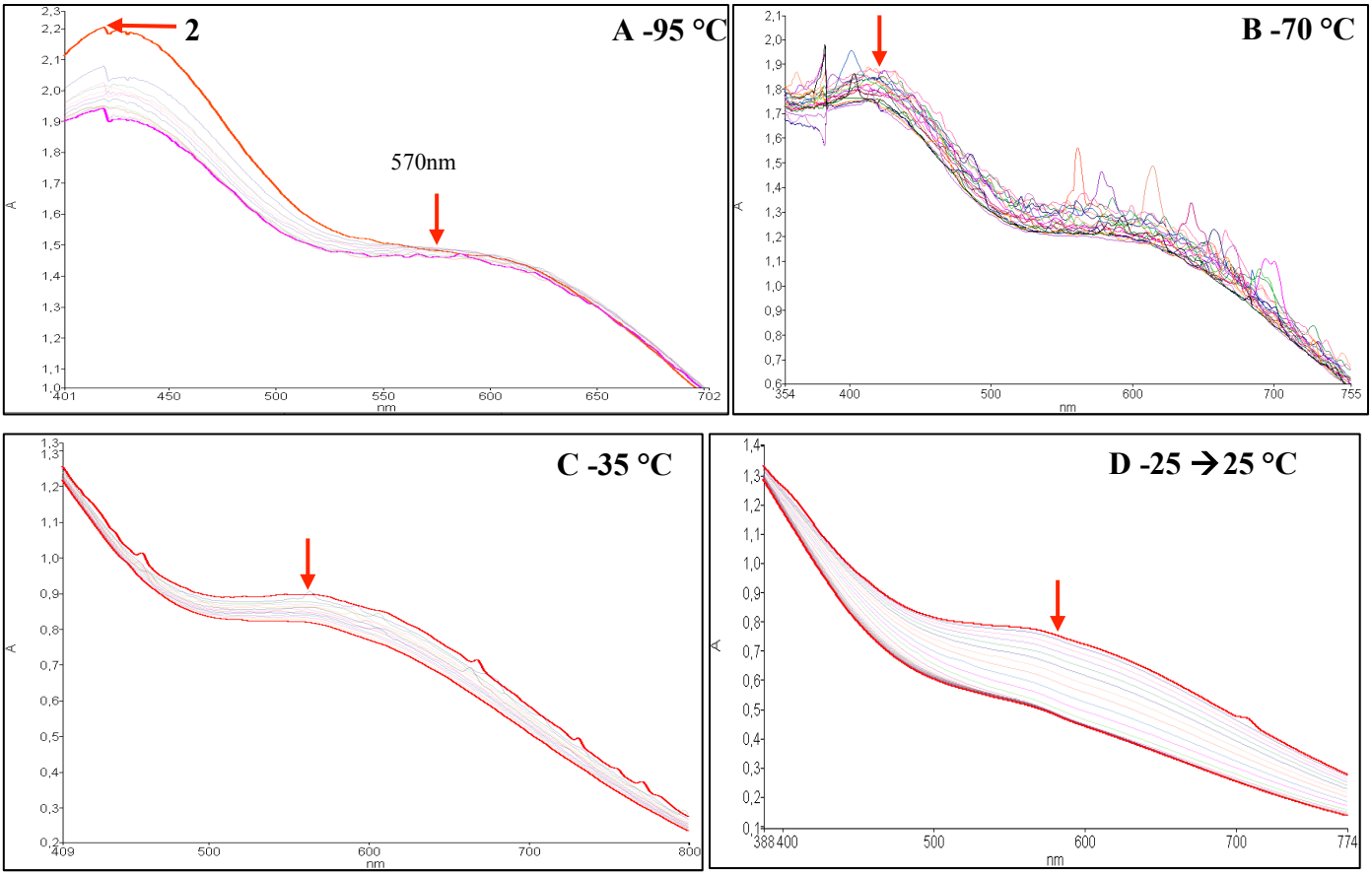

Figure S14. Compiled UV-vis spectra of the reaction between **2** and H_2hq in THF (concentration of injected H_2hq solution: 0.018 M^{-1} L^{-1}). **A**: at -95 °C for 30 min showing the presence of $[Ce(Me_2pz)_4]_2$ (**2**) and increase in turbulence. **B**: at -70 °C for one h showing turbulence from insoluble materials and loss of **2**. **C**: at -35 °C over half an h. **D**: slowly warming the sample over two h from -25 °C - 25 °C.

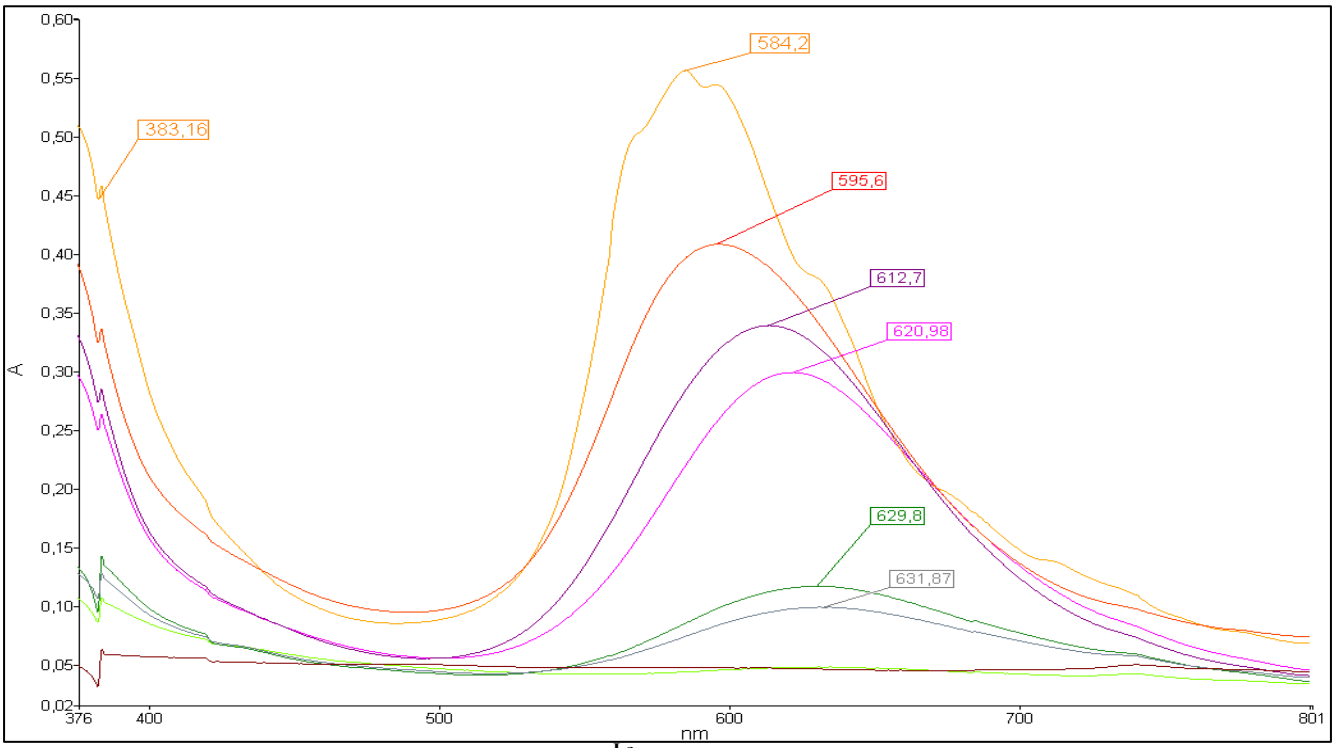

Figure S15. UV-vis spectra of the reaction between $\mathbf{1^{La}(thf)}$ (in slight excess) and bq in THF. Brown: at -95 °C prior bq addition; yellow: at -95 °C upon bq addition; orange: after 1 hour at -95 °C; purple: at -45 °C; pink: at -30 °C; green: at -10 °C; grey: at 20 °C; fluoro-green: at 50 °C.

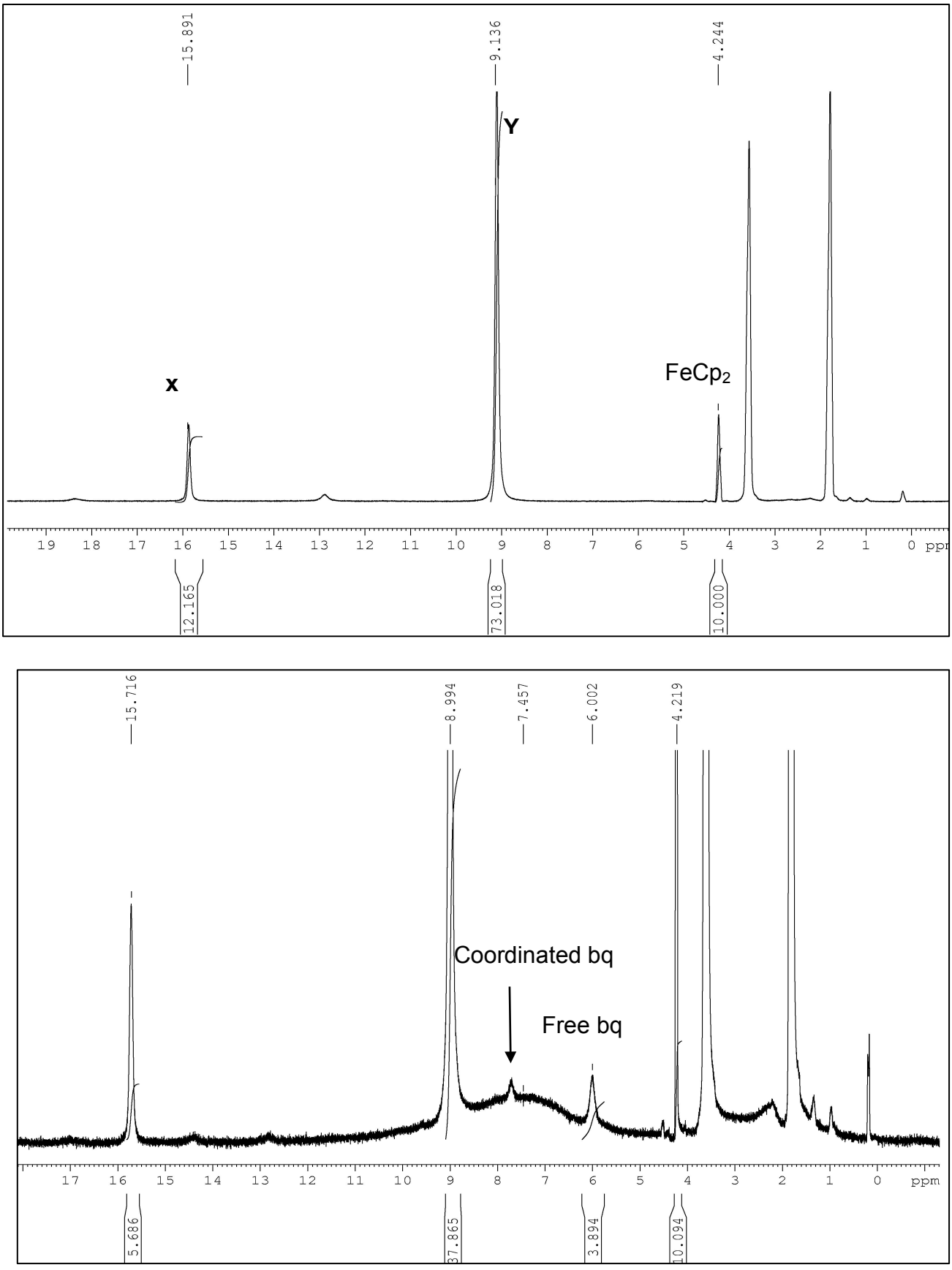

Figure S16. ^{1}H NMR spectra of $[Ce(Me_2pz)_3(thf)]_2$ (**1(thf)**) with $FeCp_2$ in THF-d_8 at 178.95 K (top; note: small resonances beyond 20 and 0 ppm were omitted); addition of bq into the solution at low temperatures (bottom).

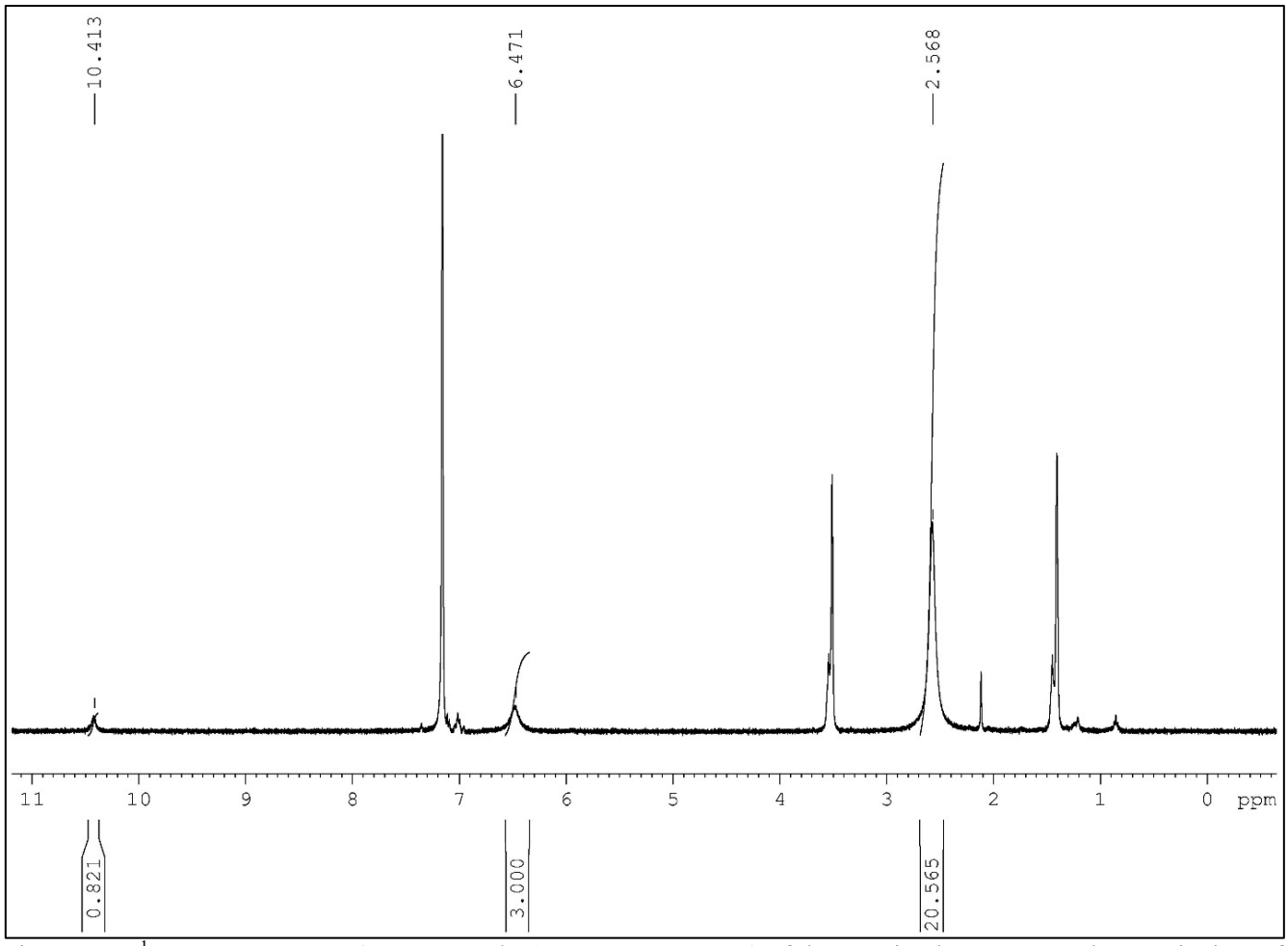

Figure S17. ^{1}H NMR spectrum (C_6D_6, THF-d_8, 400 MHz, 300.15 K) of the reaction between **2** and an equivalent of H_2hq, showing the formation of Me_2pzH.

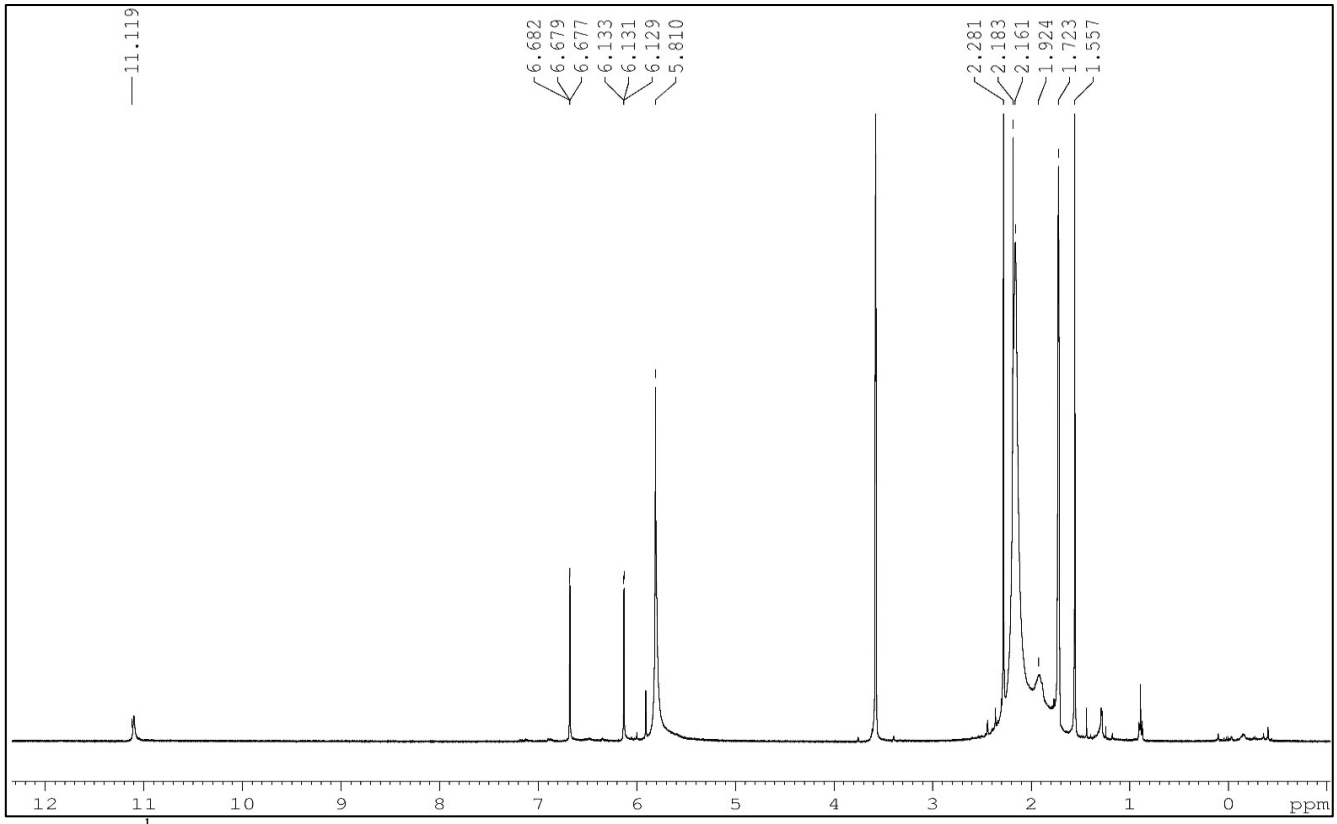

Figure S18. ^{1}H NMR spectrum (THF-d_8, 400 MHz, 300 K) of the reaction between [La(Me_2pz)$_3$] and bq, showing no clear product. Crystallisation from this mixture gave crystals of [{$La_4(Me_2pz)_7$(pchd)(pzhq)(thf-d_8)}$_2$(hq)]·4PhMe (**6a**) and [{$La_3(Me_2pz)_5$(pchd)(thf-d_8)$_X$}$_2$(hq)$_y$(pzhq)$_{2-y}$] (**6b**). Resonance at 11.12 ppm identified as "[La(Me_2pz)$_3$(Me_2pzH)]$_2$" from comparisons with the genuine sample (see Figure S31).

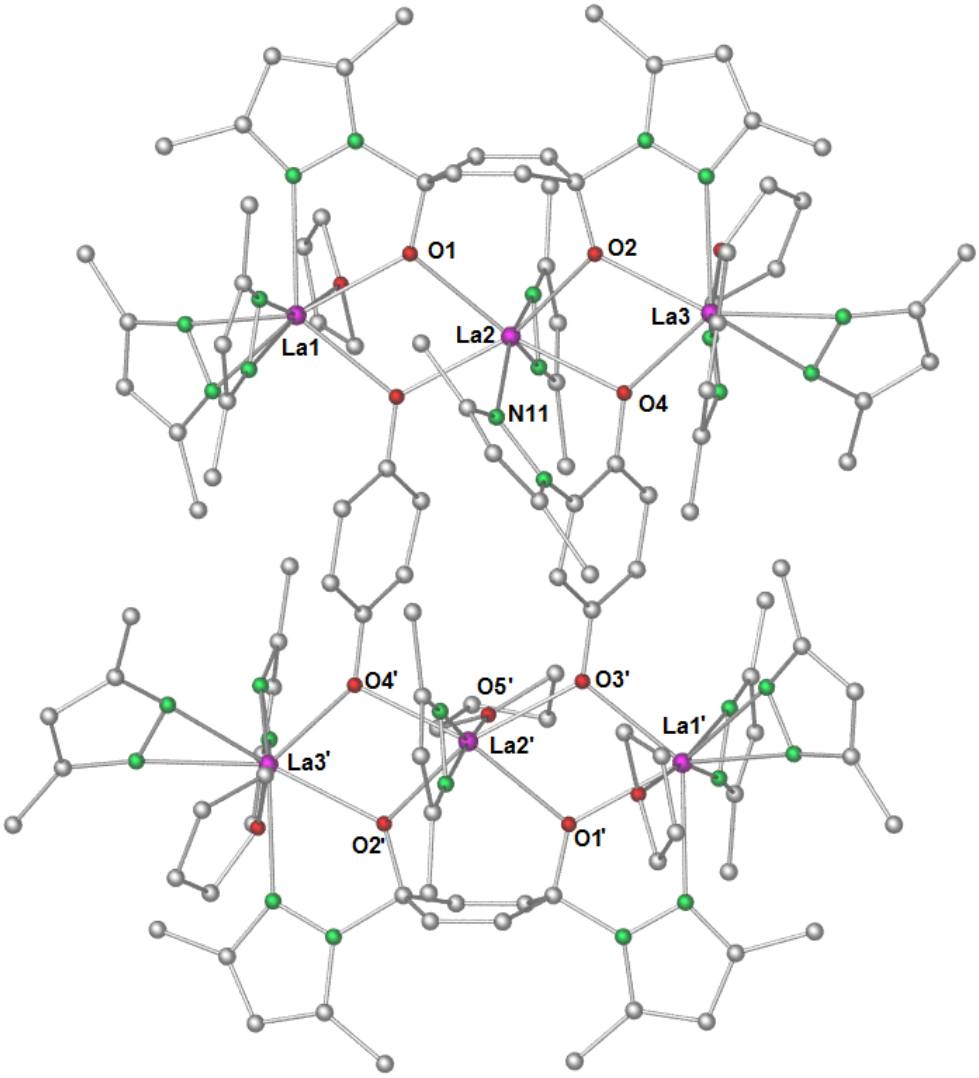

Figure S19. Molecular structure of [{$La_3(Me_2pz)_5(pchd)(thf)_{2.5}\}_2(hq)(pzhq)$] (**6c**) depicting only connectivity. For bond lengths and angles please refer to the cif file.

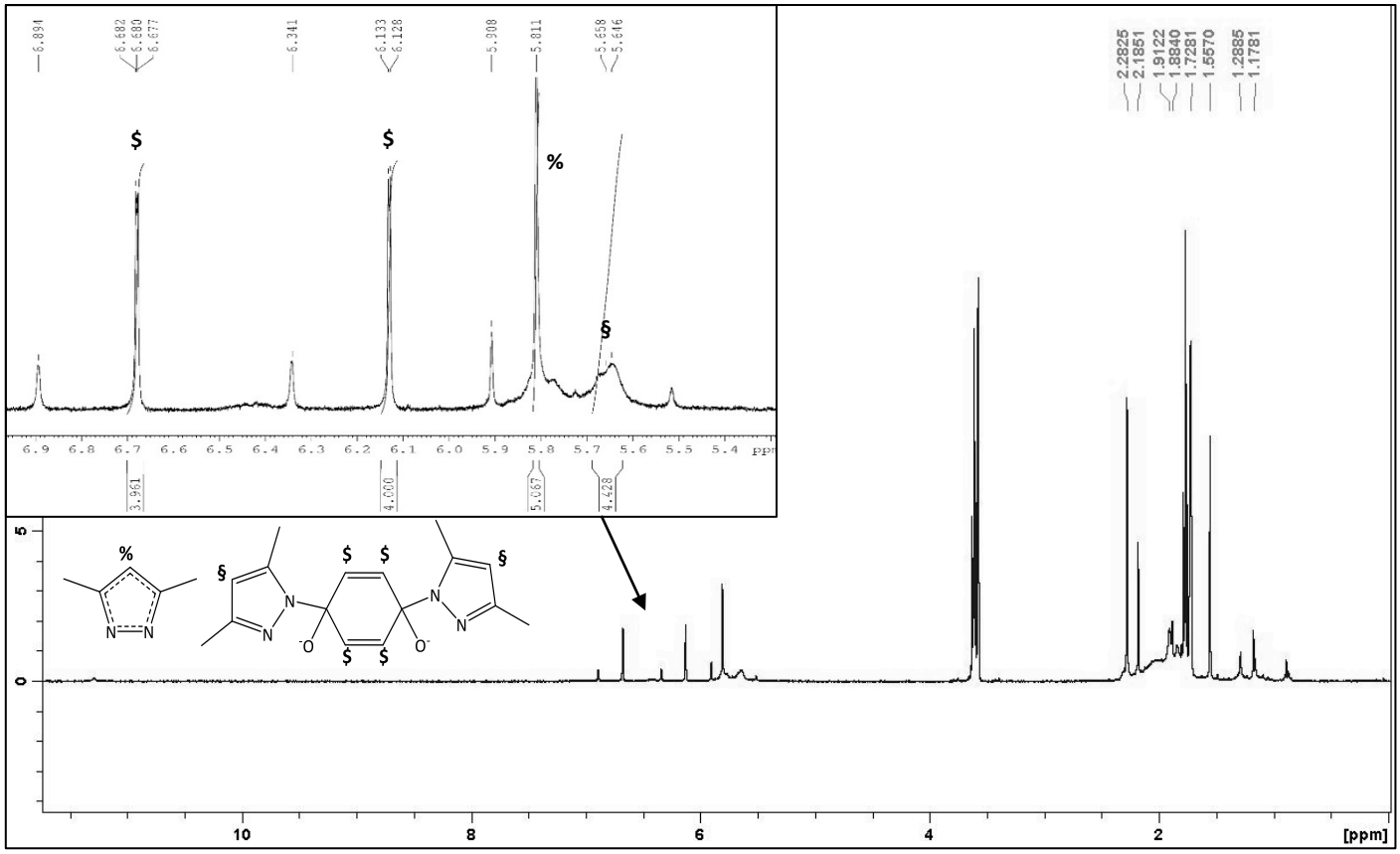

Figure S20. ^{1}H NMR spectrum (THF-d_8, 400 MHz, 300 K) of the handpicked crystals of $[La_3(Me_2pz)_5(pchd)_2(thf)_2]\cdot 2THF$ (**5a^{La}**) with small amounts of impurities, indicating the resonances responsible for the pchd component.

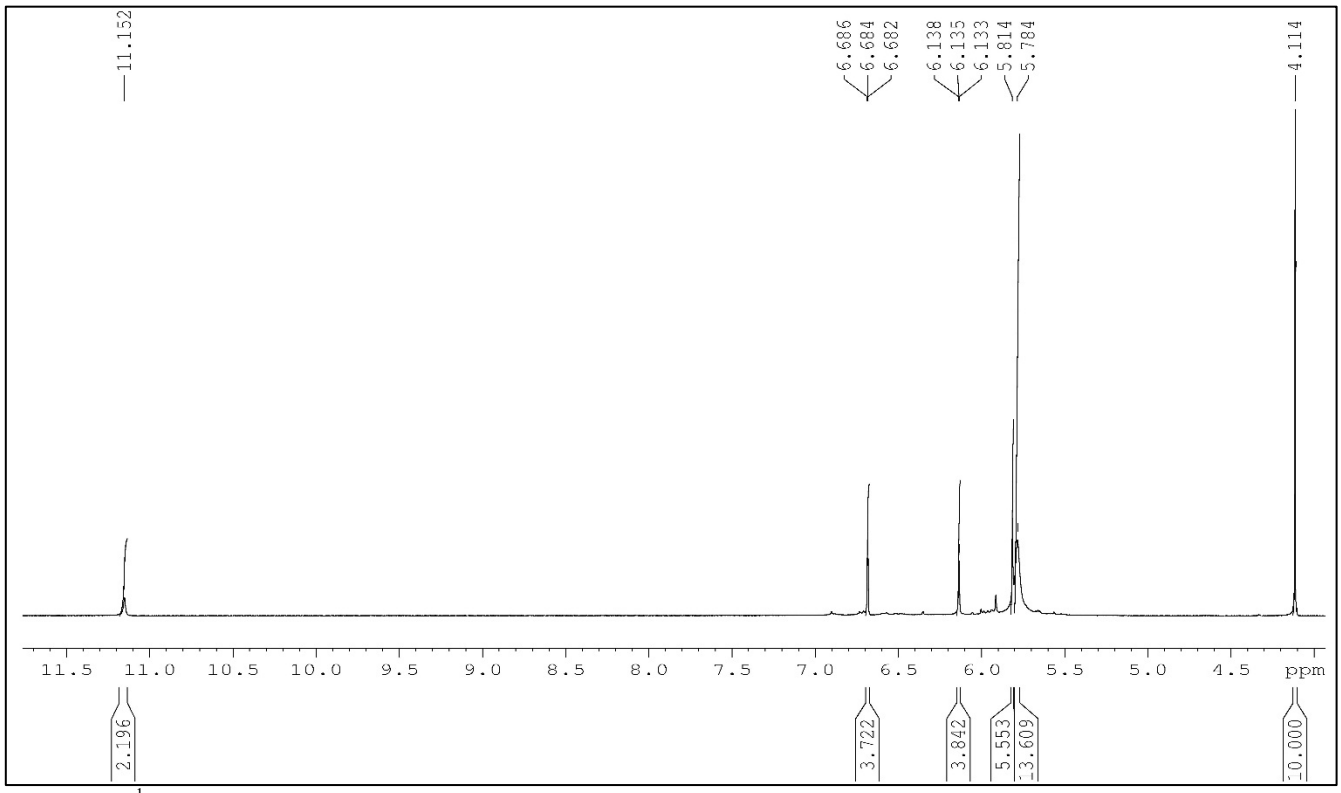

Figure S21. ^{1}H NMR spectrum (THF-d_8, 400MHz, 300 K) of the reaction between $[La(Me_2pz)_3(thf)]_2$ and bq with $FeCp_2$ the ratio used were 7:3:1 respectively.

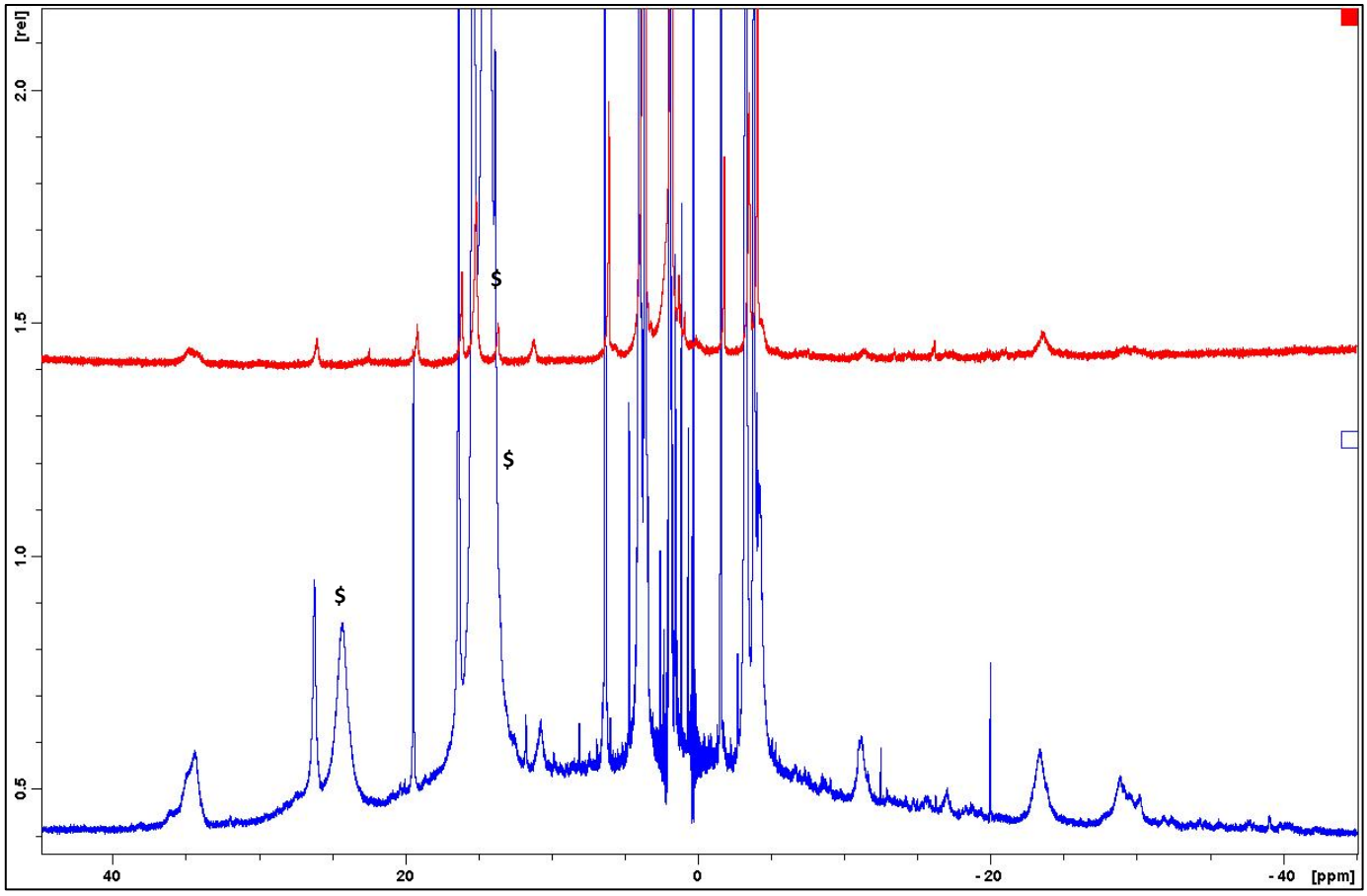

Figure S22. Stacked ^{1}H NMR spectra (THF-d_8, 400MHz, 300 K) of isolated $[Pr_3(Me_2pz)_5(pchd)_2(thf)_2]\cdot 2THF$ (**5a^{Pr}**, red top containing minimal amounts of **6c^{Pr}**) and the reaction mixture between $[Pr(Me_2pz)_3(thf)]_2$ **1^{Pr}(thf)** and bq in THF-d_8 ($ -**1^{Pr}(thf)**) showing the broadened baseline from other paramagnetic species.

Other relevant spectra for reported complexes

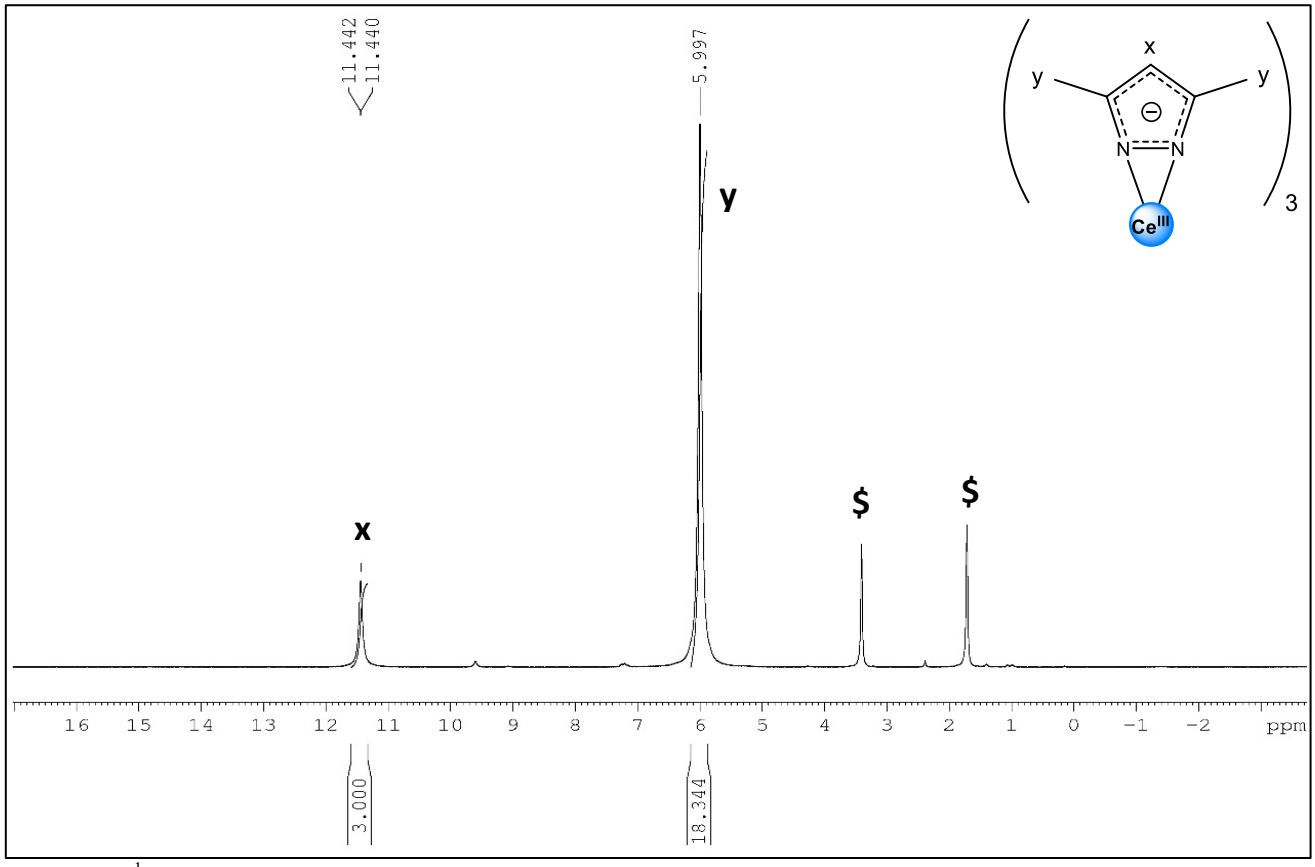

Figure S23. ^{1}H NMR (400 MHz) spectrum of [Ce(Me$_2$pz)$_3$] (**1**) in THF-d$_8$ at 300 K ($ = THF-d$_8$).

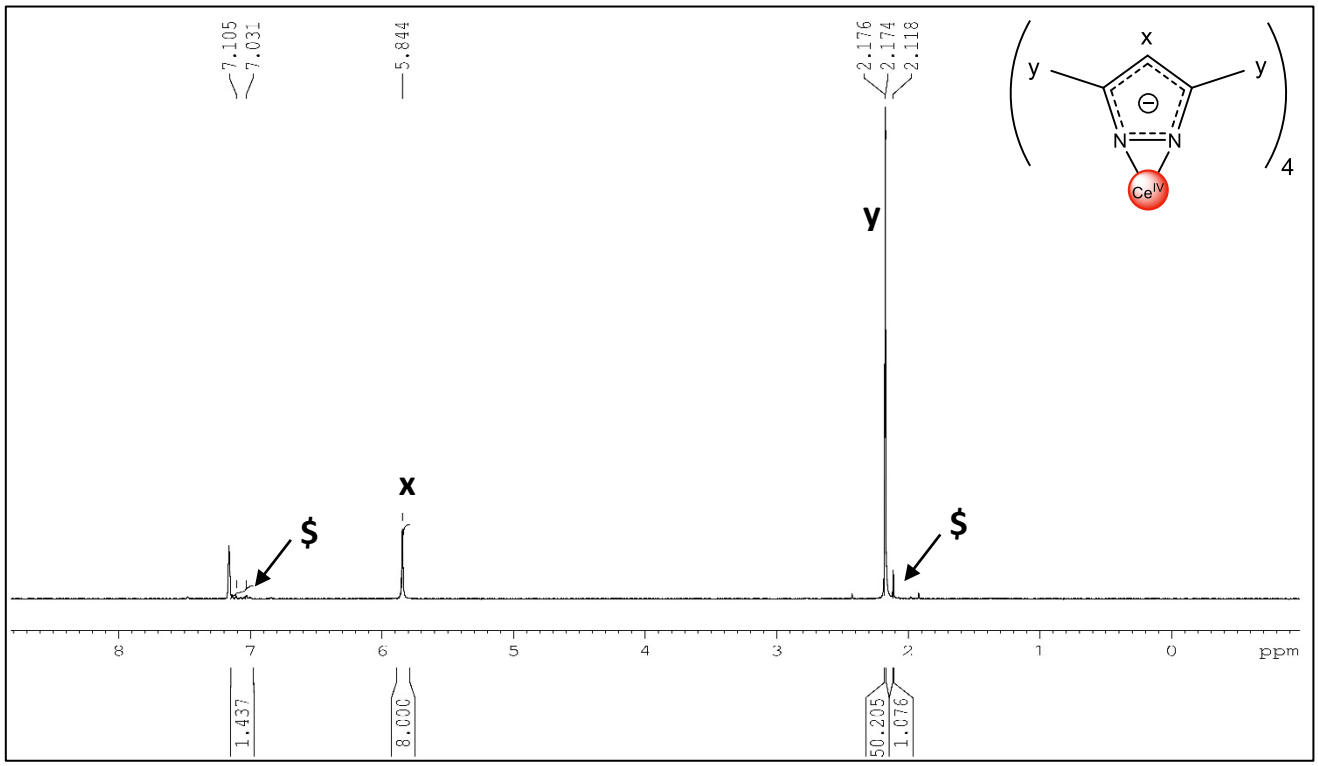

Figure S24. ^{1}H NMR (250 MHz) spectrum of [Ce(Me$_2$pz)$_4$]$_2$·$^{1}/_{4}$PhMe (**2**·$^{1}/_{4}$PhMe) in C$_6$D$_6$ at 300 K ($ = toluene).

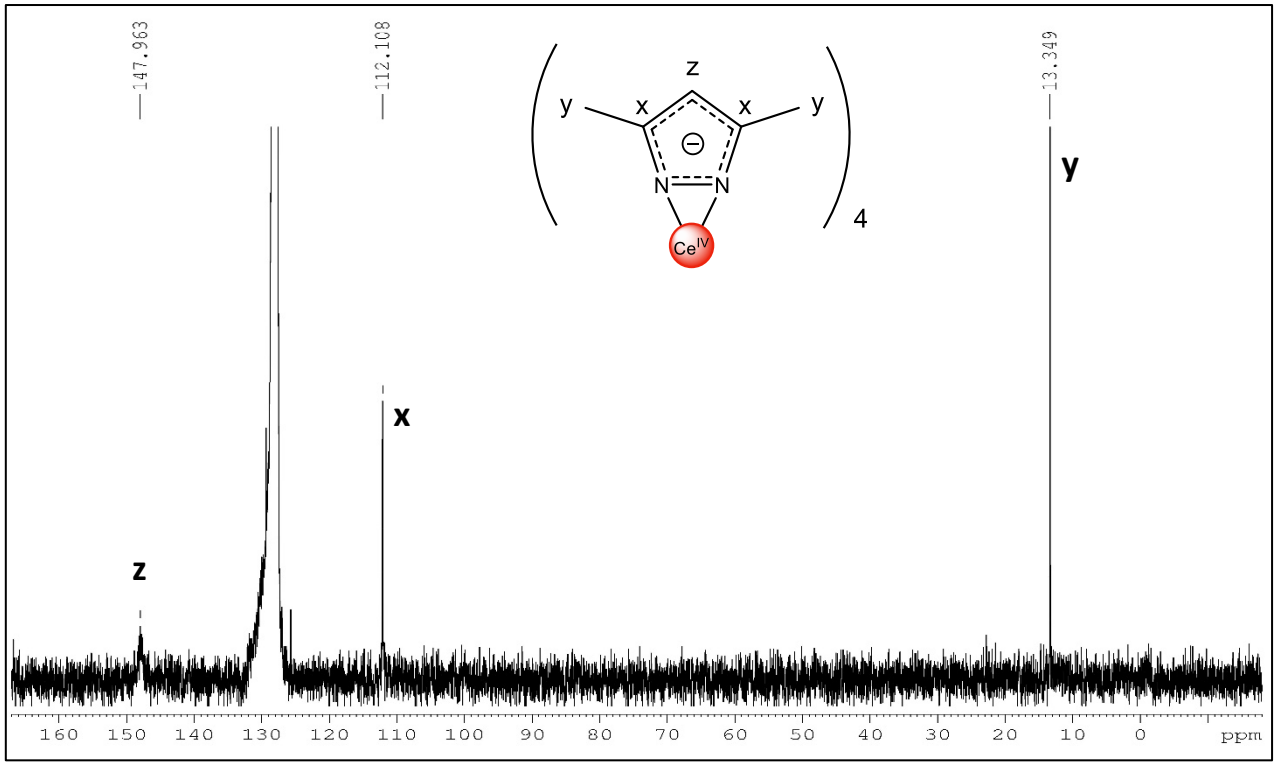

Figure S25. ^{13}C NMR (63 MHz) spectrum of $[Ce(Me_2pz)_4]_2 \cdot {}^1/_4PhMe$ (**2**$\cdot {}^1/_4PhMe$) in C_6D_6 at 300 K.

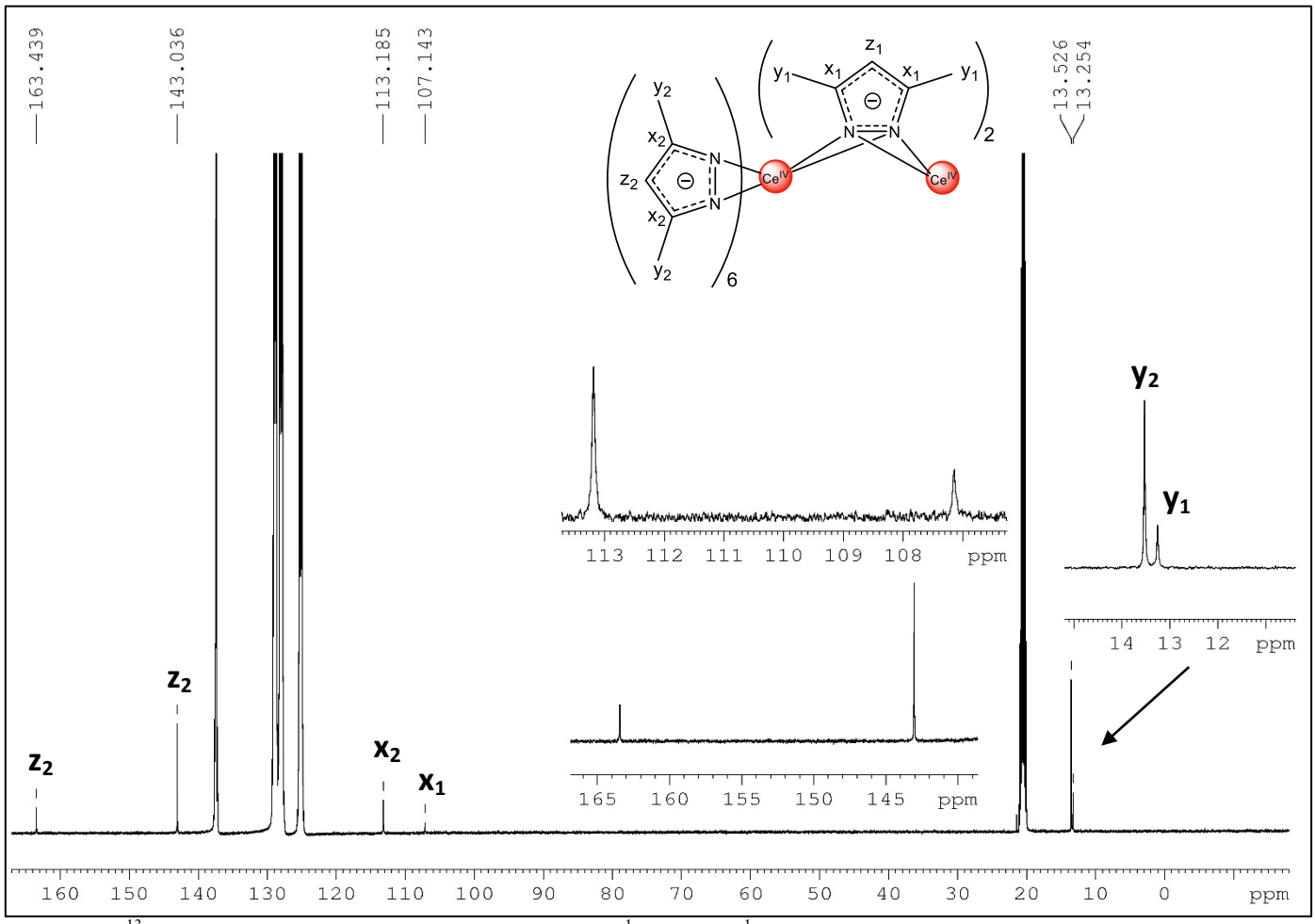

Figure S26. ^{13}C NMR (125 MHz) spectrum of $[Ce(Me_2pz)_4]_2 \cdot {}^1/_4PhMe$ (**2**$\cdot {}^1/_4PhMe$) in toluene-d_8 at 193 K.

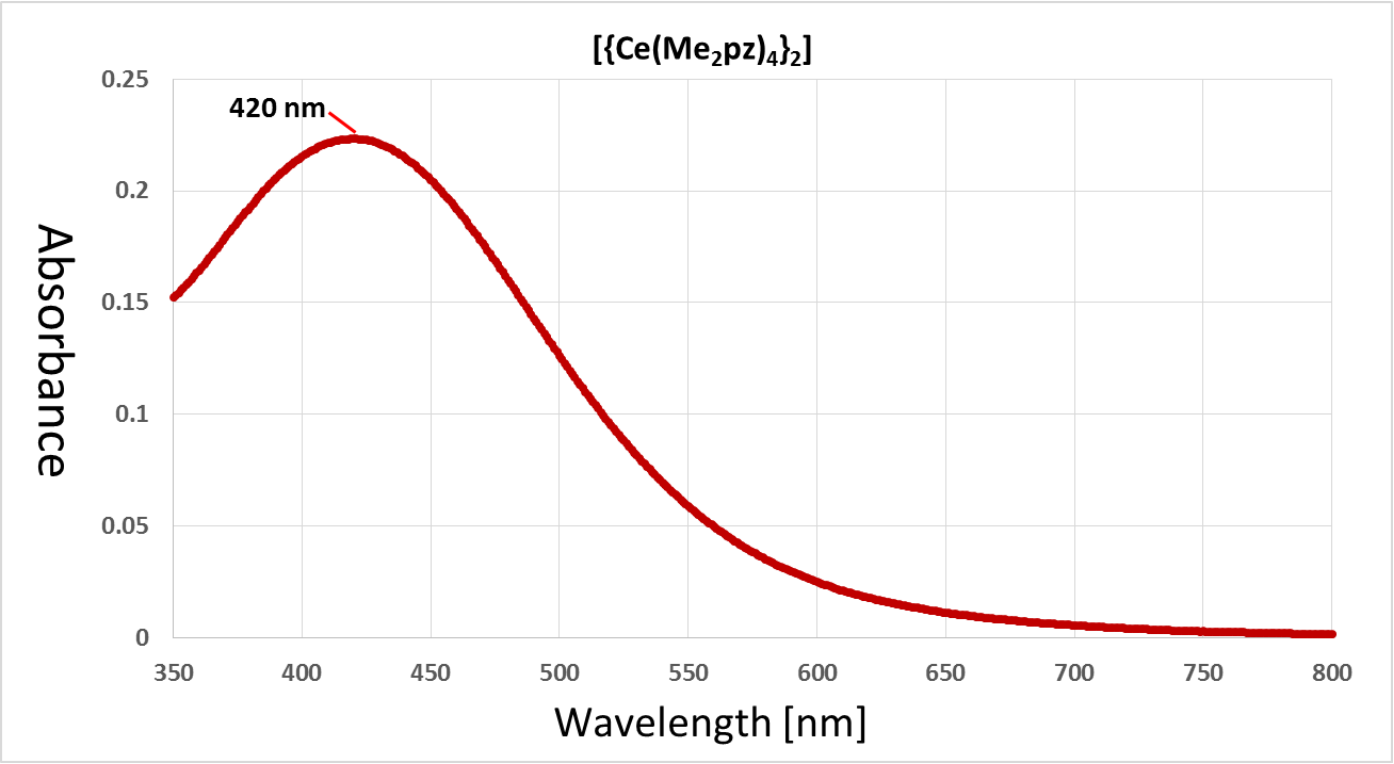

Figure S27. UV-vis spectrum of $[Ce(Me_2pz)_4]_2$ (**2**) in toluene at ambient temperature.

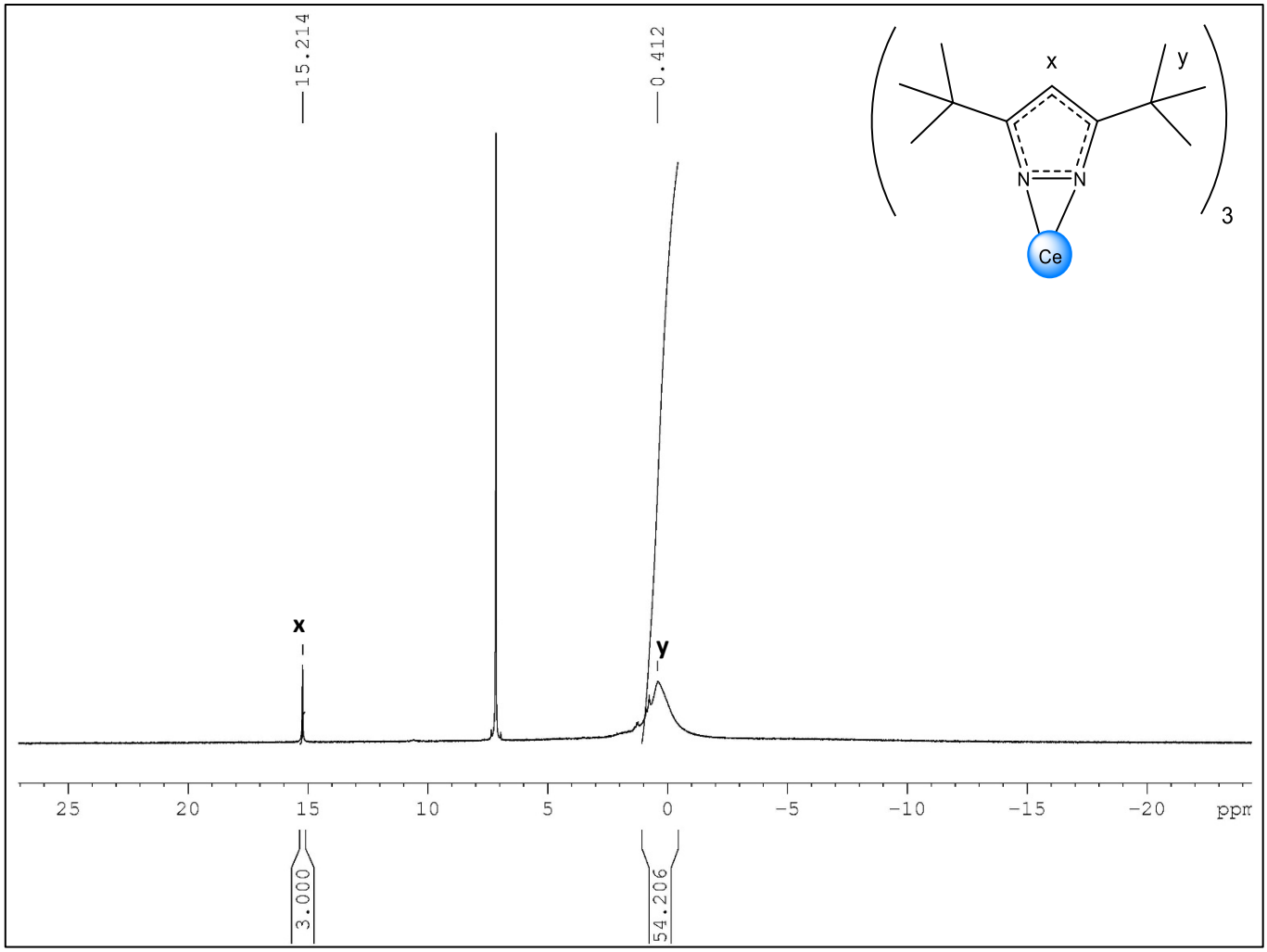

Figure S28. ^{1}H NMR (400 MHz, C_6D_6, 300 K) spectrum of $[Ce(t\text{Bu}_2\text{pz})_3]_2$ (**3**).

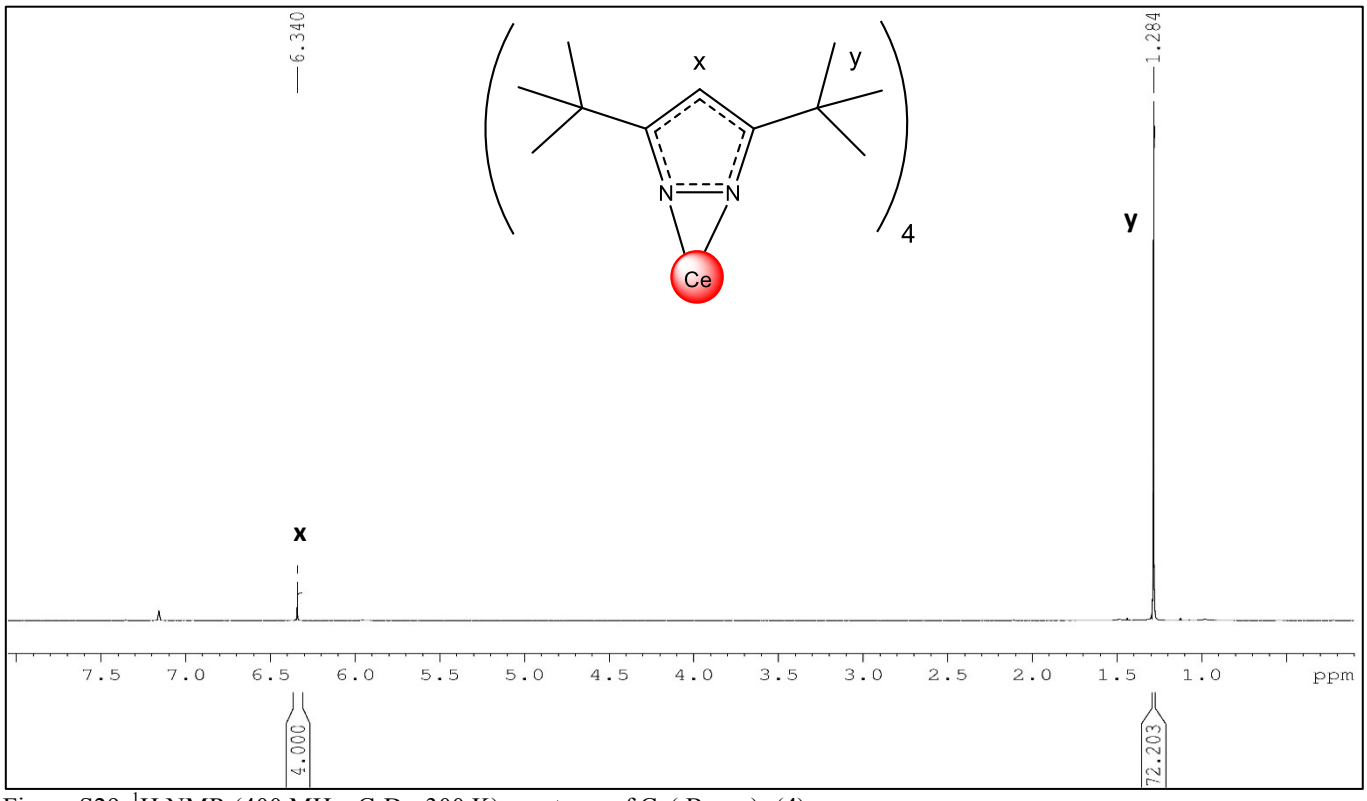

Figure S29. ^{1}H NMR (400 MHz, C_6D_6, 300 K) spectrum of $Ce(t\text{Bu}_2\text{pz})_4$ (**4**).

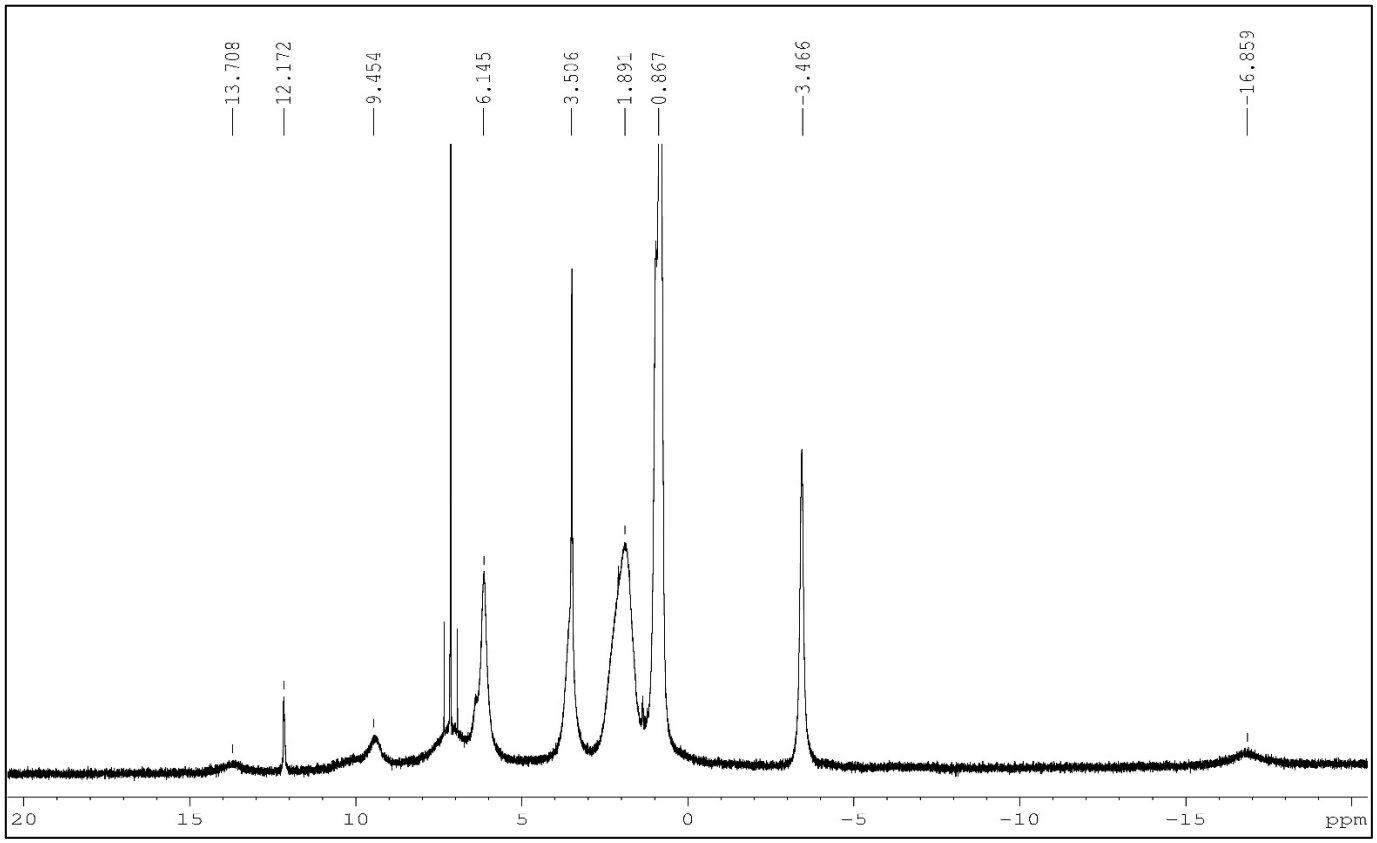

Figure S30. ^{1}H NMR (400 MHz) spectrum of [$Ce_3(Me_2pz)_5(pchd)_2(thf)$] (**5a** – thf) in C_6D_6 at 300 K. The sample was poorly soluble, and due to paramagnetic broadening no meaningful integrations/assignments were obtained.

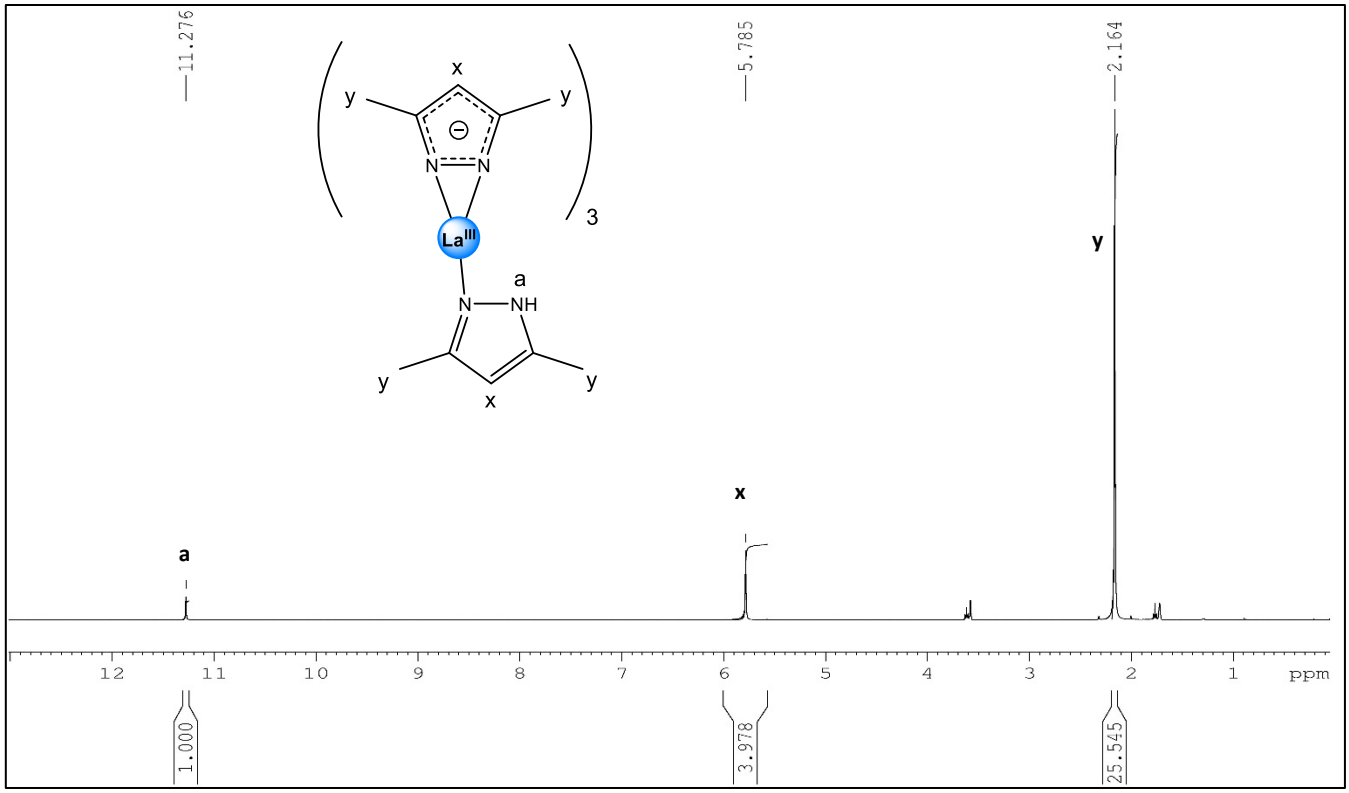

Figure S31. ^{1}H NMR spectrum (THF-d_8, 400MHz, 300 K) of [$La(Me_2pz)_3(Me_2pzH)]_2$.

Additional X-ray crystallographic details

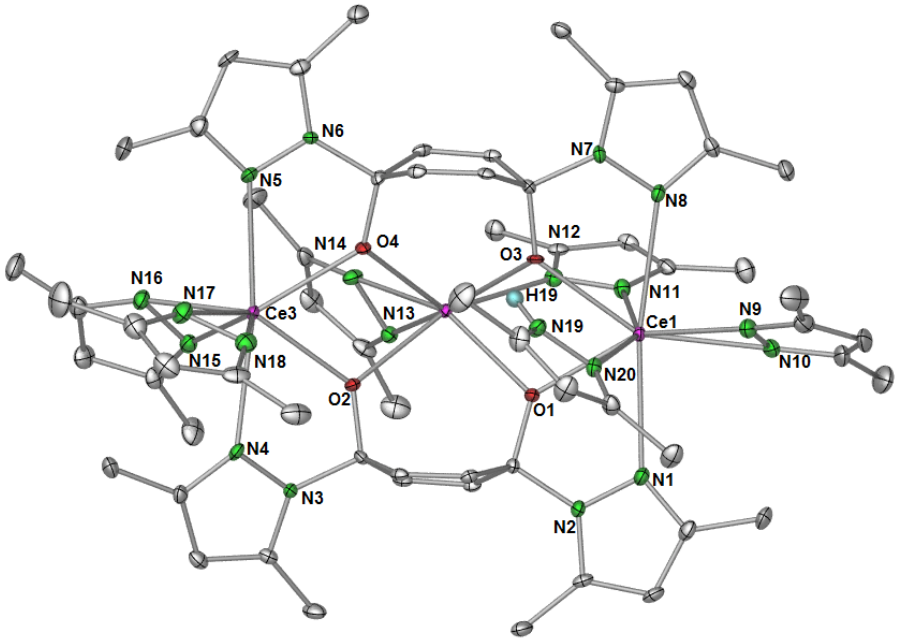

Figure S32. Molecular structure of $[Ce_3(Me_2pz)_5(pchd)_2(Me_2pzH)]$ (**5b**). Ellipsoids are shown at 50% probability and hydrogen atoms (except H19) have been removed for clarity. For bond lengths and angles please refer to Table S4 below.

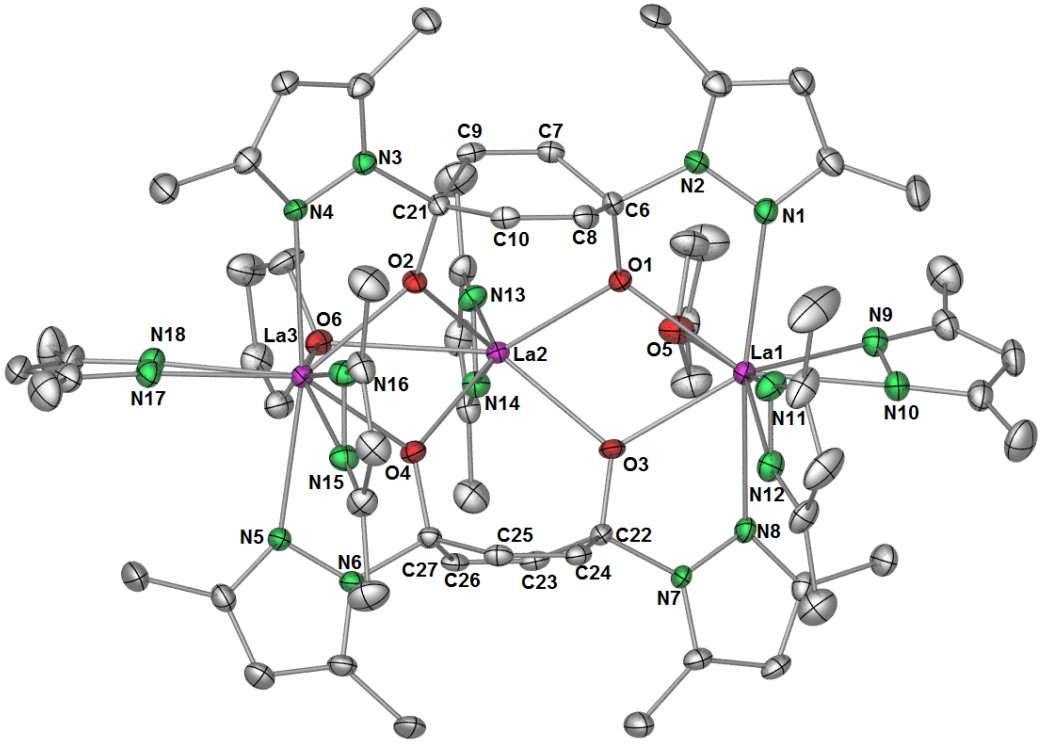

Figure S33. Molecular structure of $[La_3(Me_2pz)_5(pchd)_2(thf)_2]\cdot 2THF$ (**5a**^{La}). For bond lengths and angles please refer to Table S5.

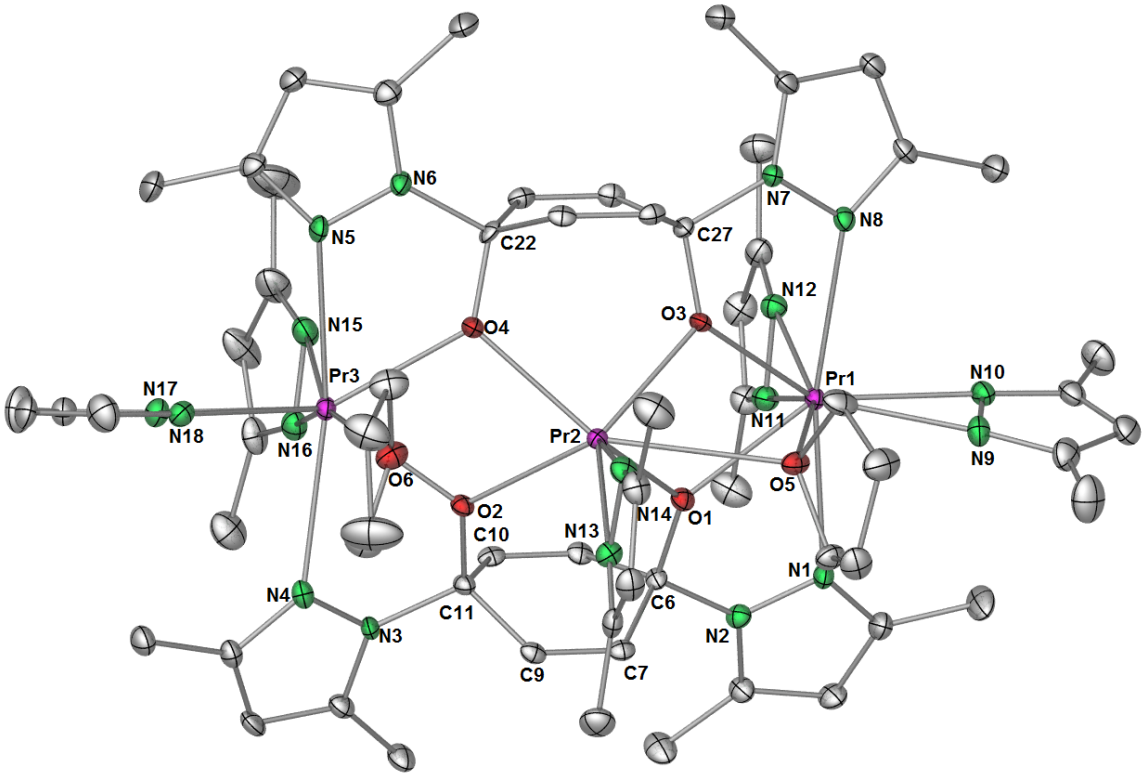

Figure S34. Molecular structure of $[Pr_3(Me_2pz)_5(pchd)_2(thf)_2]\cdot 2THF$ (**5a**^{Pr}). For bond lengths and angles please refer to Table S6.

Table S1. Selected bond lengths (Å) for $[Ce(Me_2pz)_4]_2$ (**2**)

Bond		(Å)	Bond		(Å)
Ce1	N1	2.384(2)	Ce2	N7	2.473(2)
Ce1	N2	2.368(3)	Ce2	N8	2.531(3)
Ce1	N3	2.342(3)	Ce2	N9	2.693(2)
Ce1	N4	2.382(2)	Ce2	N10	2.591(2)
Ce1	N5	2.319(3)	Ce2	N11	2.400(2)
Ce1	N6	2.369(3)	Ce2	N12	2.351(3)
Ce1	N7	2.708(2)	Ce2	N13	2.373(3)
Ce1	N8	2.671(3)	Ce2	N14	2.367(2)
Ce1	N9	2.475(2)	Ce2	N15	2.311(2)
Ce1	N10	2.529(2)	Ce2	N16	2.370(3)

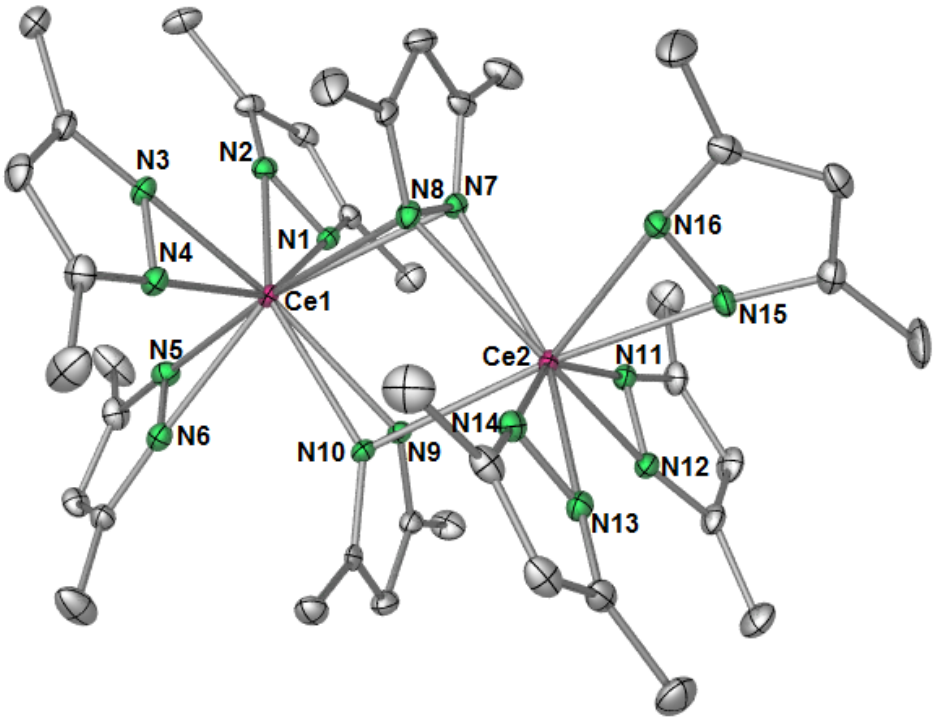

Table S2. Selected bond lengths for $Ce(tBu_2pz)_4$ (**4**)

Bond		Å
Ce1	N1	2.343 (4)
Ce1	N2	2.356 (4)
Ce1	N3	2.322(4)
Ce1	N4	2.350(4)
Ce1	N5	2.348(4)
Ce1	N6	2.359(5)
Ce1	N7	2.365(4)
Ce1	N8	2.350(4)

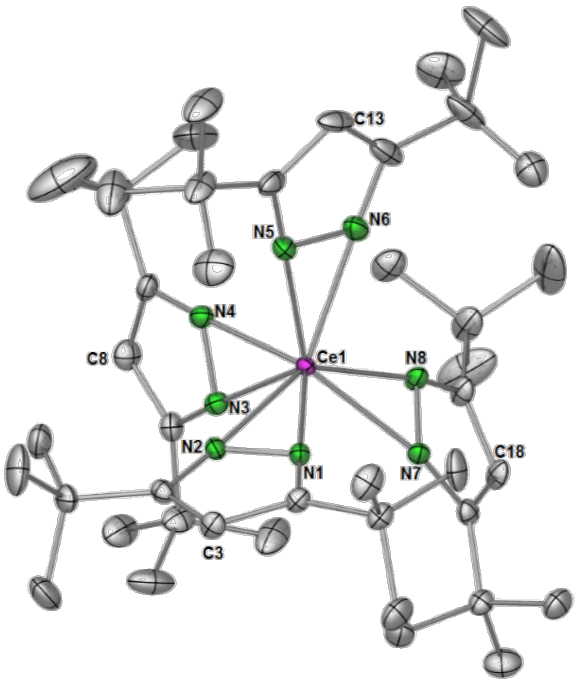

Atoms	Angle (°)	Atoms	Angle (°)
C3-Ce1-C8	113.41(10)	C3-Ce1-C13	99.15(10)
C3-Ce1-C18	118.48(10)	C8-Ce1-C13	113.92(10)
C8-Ce1-C18	88.43(11)	C13-Ce1-C18	124.16(11)

Table S3. Selected bond lengths (°) and angles (Å) for $[Ce_3(Me_2pz)_5(pchd)_2(thf\text{-}d_8)_2]$ (**5a**)

Bond		Å
Ce1	O1	2.450(3)
Ce1	O3	2.474(3)
Ce1	O5	2.623(3)
Ce1	N1	2.724(4)
Ce1	N8	2.692(4)
Ce1	N9	2.565(4)
Ce1	N10	2.443(4)
Ce1	N11	2.477(4)
Ce1	N12	2.476(4)
Ce2	Ce3	3.9534(4)
Ce2	O1	2.400(3)
Ce2	O2	2.403(3)
Ce2	O3	2.421(3)
Ce2	O4	2.433(3)
Ce2	O6	2.894(3)
Ce2	N13	2.460(3)
Ce2	N14	2.507(4)
Ce3	O2	2.443(3)
Ce3	O4	2.436(3)
Ce3	O6	2.864(3)
Ce3	N4	2.694(4)
Ce3	N5	2.732(4)
Ce3	N15	2.468(4)
Ce3	N16	2.496(4)
Ce3	N17	2.489(4)
Ce3	N18	2.539(4)
O1	C6	1.381(5)
C6	N2	1.488(5)
N2	N1	1.380(5)

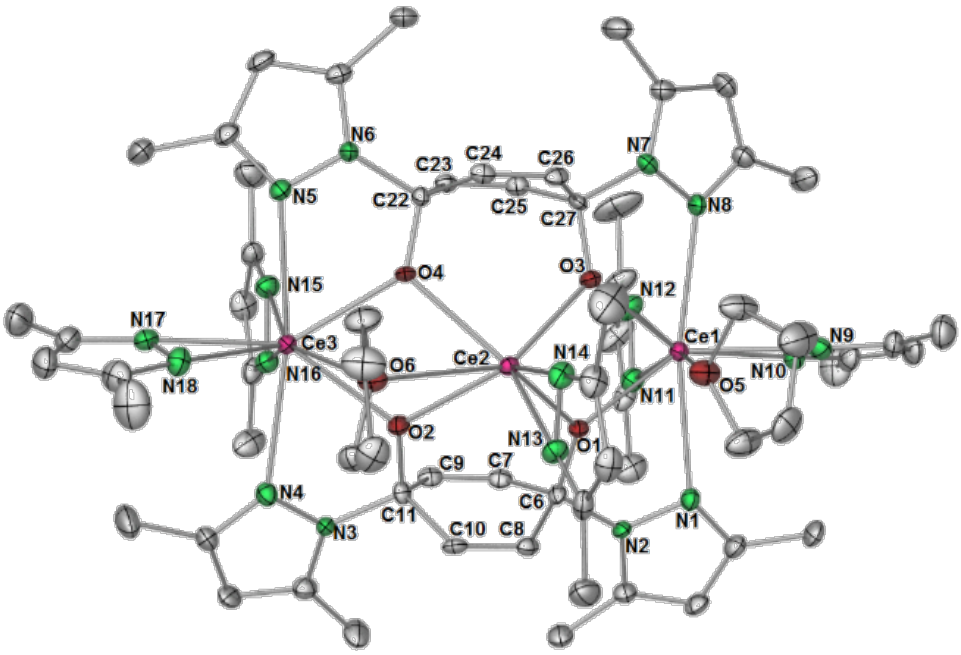

Atoms	Angle (°)	Atoms	Angle (°)
Ce1-O1-Ce2	110.97(11)	Ce1-O1-Ce2	110.97(11)
Ce1-O1-C6	125.3(3)	Ce1-N1-N2	110.0(3)
O1-Ce2-O2	86.87(10)	Ce2-O1-C6	123.4(2)
Ce2-O2-C11	122.6(2)	O1-Ce2-O4	128.32(10)
Ce2-O2-Ce3	109.33(11)	Ce3-O2-C11	128.0(3)
O2-Ce3-N4	61.20(11)	Ce3-N4-N3	113.4(3)

Bond		Å
C6	C7	1.506(6)
C7	C9	1.325(6)
C9	C11	1.525(6)
C11	O2	1.384(5)
C11	C10	1.512(6)
C10	C8	1.328(6)
C11	N3	1.496(5)
N3	N4	1.352(5)

Table S4. Bond lengths (Å) and angles (°) for complex $[Ce_3(Me_2pz)_5(pchd)_2(Me_2pzH)]$ (**5b**)

Bond		Å	Bond		Å	Atoms	Angle (°)
Ce1	O1	2.399(2)	Ce2	N12	2.629(3)	Ce1-O1-Ce2	108.77(9)
Ce1	O3	2.446(2)	Ce2	N13	2.439(3)	Ce1-O1-C6	132.3(2)
Ce1	N1	2.710(3)	Ce2	N14	2.493(3)	Ce1-N1-N2	115.67(19)
Ce1	N8	2.714(3)	Ce3	O2	2.421(2)	O1-Ce1-O3	67.65(7)
Ce1	N9	2.428(3)	Ce3	O4	2.430(2)	Ce2-O1-C6	118.95(19)
Ce1	N10	2.527(3)	Ce3	N4	2.661(3)	O1-Ce2-O2	88.82(2)
Ce1	N11	2.588(3)	Ce3	N5	2.642(3)	01-Ce2-O4	121.95(7)
Ce1	N20	2.671(3)	Ce3	N15	2.436(3)	Ce2-O2-C11	120.22(18)
Ce2	O1	2.459(2)	Ce3	N16	2.533(3)	Ce3-O2-C11	130.07(18)
Ce2	O2	2.428(2)	Ce3	N17	2.485(3)	O2-Ce3-N4	61.91(8)
Ce2	O3	2.556(2)	Ce3	N18	2.518(3)	Ce3-N4-N3	116.3(2)
Ce2	O4	2.466(2)				Ce2-O2-Ce3	109.70(9)

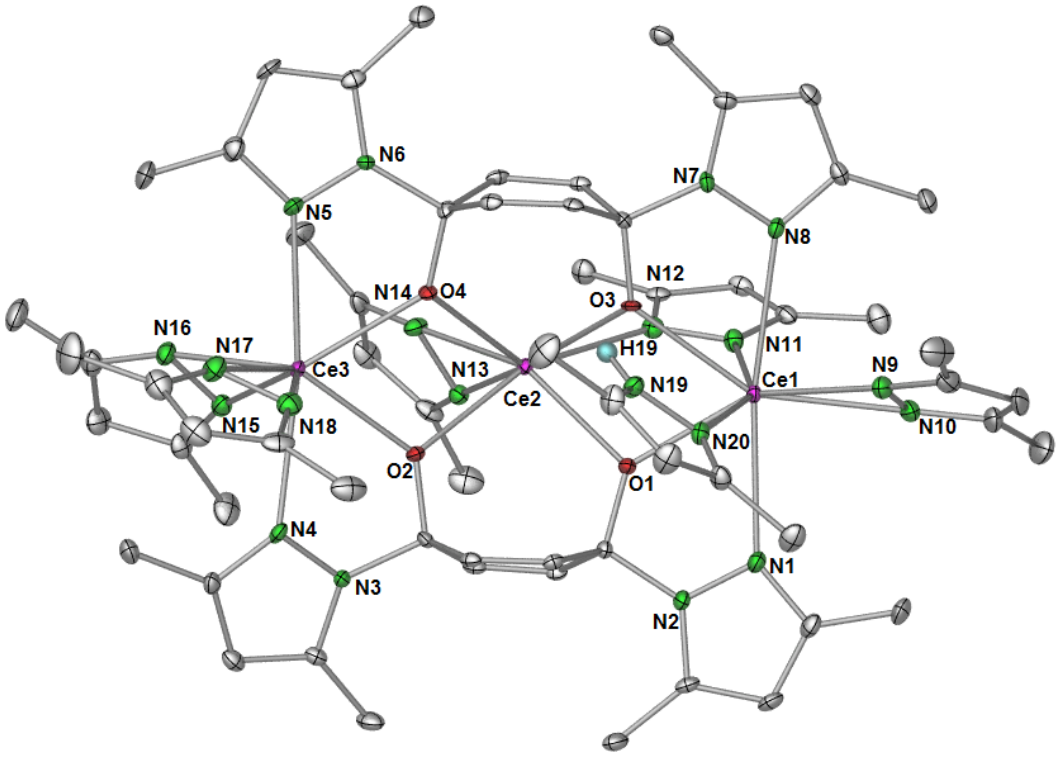

Table S5. Bond lengths (Å) and angles (°) for complex $[La_3(Me_2pz)_5(pchd)_2(thf)_2]\cdot 2THF$ (**5a**^{La})

Bond		Å
La1	O1	2.497(2)
La1	O3	2.469(2)
La1	O5	2.666(3)
La1	N1	2.714(3)
La1	N8	2.743(3)
La1	N9	2.577(3)
La1	N10	2.473(3)
La1	N11	2.494(4)
La1	N12	2.500(3)
La2	La3	3.9940(3)
La2	O1	2.451(2)
La2	O2	2.451(2)
La2	O3	2.426(3)
La2	O4	2.436(2)
La2	O6	2.901(3)
La2	N13	2.535(3)
La2	N14	2.488(3)
La3	O2	2.461(2)
La3	O4	2.461(2)
La3	O6	2.880(3)
La3	N4	2.757(3)
La3	N5	2.711(3)
La3	N15	2.518(3)
La3	N16	2.501(3)
La3	N17	2.524(3)
La3	N18	2.559(3)
O1	C6	1.391(4)
C6	N2	1.498(4)
N2	N1	1.369(4)

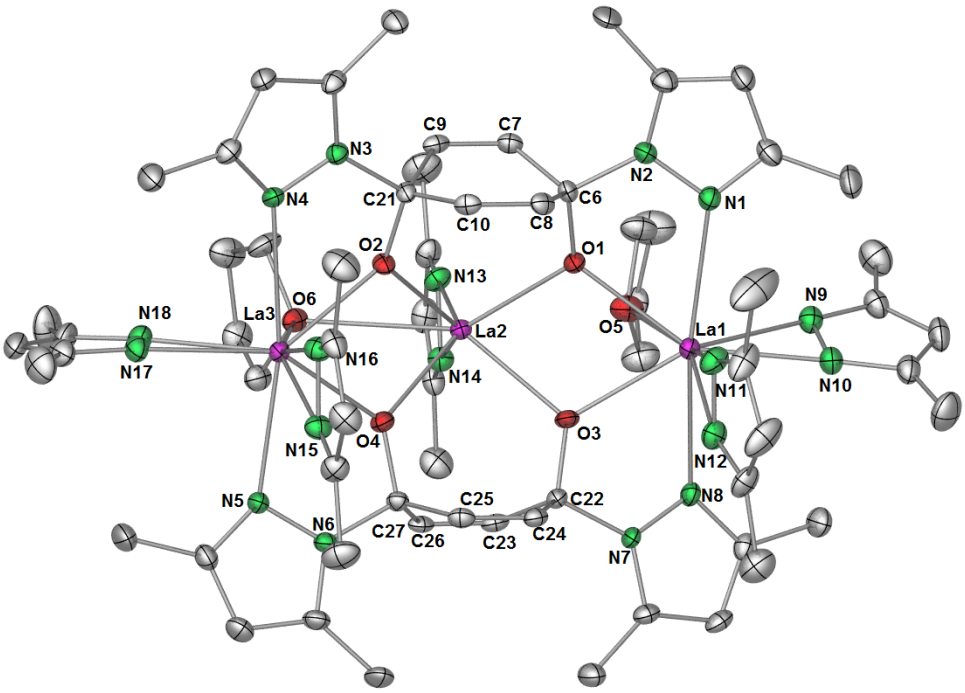

Atoms		Angle (°)
La1-O1-La2		108.83(9)
La1-O1-C6		129.6(2)
O1-La2-O2		87.67(8)
La2-O2-C21		121.00(19)
La2-O2-La3		108.58(9)
O2-La3-N4		60.47(9)
Bond		**Å**
C6	C7	1.518(5)
C7	C9	1.313(5)
C9	C21	1.523(5)
C21	O2	1.390(4)
C21	C10	1.507(5)
C10	C8	1.332(5)
C21	N3	1.500(4)
N3	N4	1.370(4)

Table S6. Bond lengths (Å) and angles (°) for complex $[Pr_3(Me_2pz)_5(pchd)_2(thf)_2]\cdot 2THF$ (**5a^{Pr}**)

Bond		Å
Pr1	O1	2.429(2)
Pr1	O3	2.423(2)
Pr1	O5	2.884(3)
Pr1	N1	2.678(3)
Pr1	N8	2.715(3)
Pr1	N9	2.520(3)
Pr1	N10	2.471(3)
Pr1	N11	2.467(3)
Pr1	N12	2.449(3)
Pr2	Pr3	3.9706(3)
Pr2	O1	2.386(2)
Pr2	O2	2.377(3)
Pr2	O3	2.405(2)
Pr2	O4	2.403(2)
Pr2	O6	2.600(2)
Pr2	N13	2.437(3)
Pr2	N14	2.492(3)
Pr3	O2	2.435(2)
Pr3	O4	2.460(3)
Pr3	O6	2.600(2)
Pr3	N4	2.708(3)
Pr3	N5	2.674(3)
Pr3	N15	2.449(3)
Pr3	N16	2.458(3)
Pr3	N17	2.430(3)
Pr3	N18	2.533(3)
O1	C6	1.388(4)
C6	N2	1.484(4)
N2	N1	1.363(4)

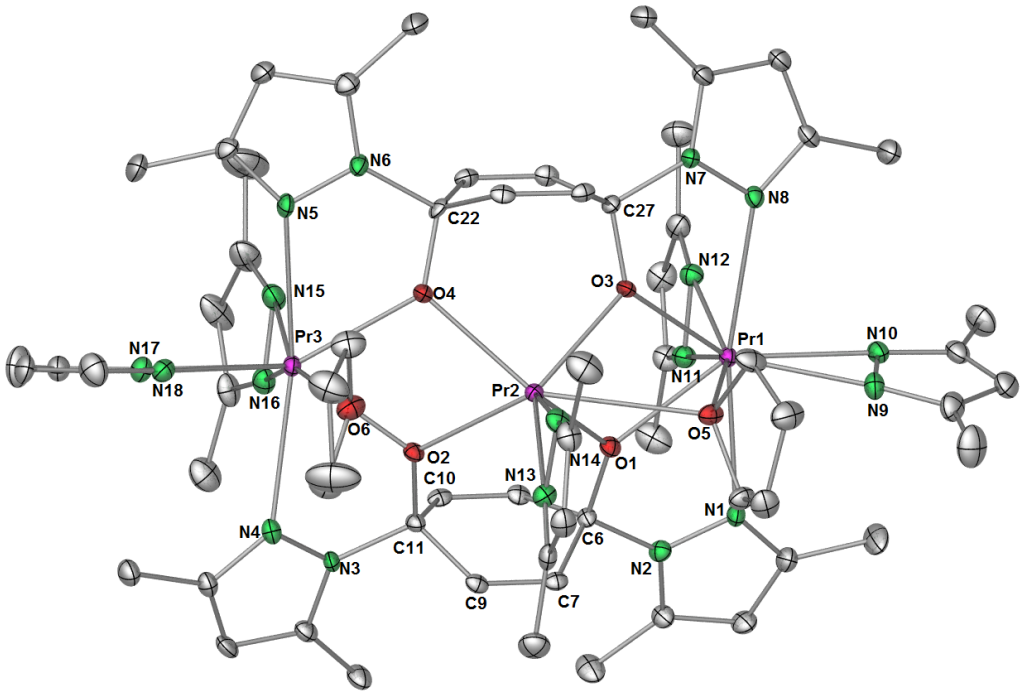

Atoms		Angle (°)
Pr1-O1-Pr2		108.93(10)
Pr1-O1-C6		127.9(2)
O1-Pr2-O2		87.21(8)
Pr2-O2-C11		123.4(2)
Pr2-O2-Pr3		111.20(9)
O2-Pr3-N4		61.07(9)
Bond		**Å**
C6	C7	1.518(5)
C7	C9	1.324(5)
C9	C11	1.517(5)
C11	O2	1.390(4)
C11	C10	1.524(5)
C10	C8	1.319(5)
C11	N3	1.490(4)
N3	N4	1.373(4)

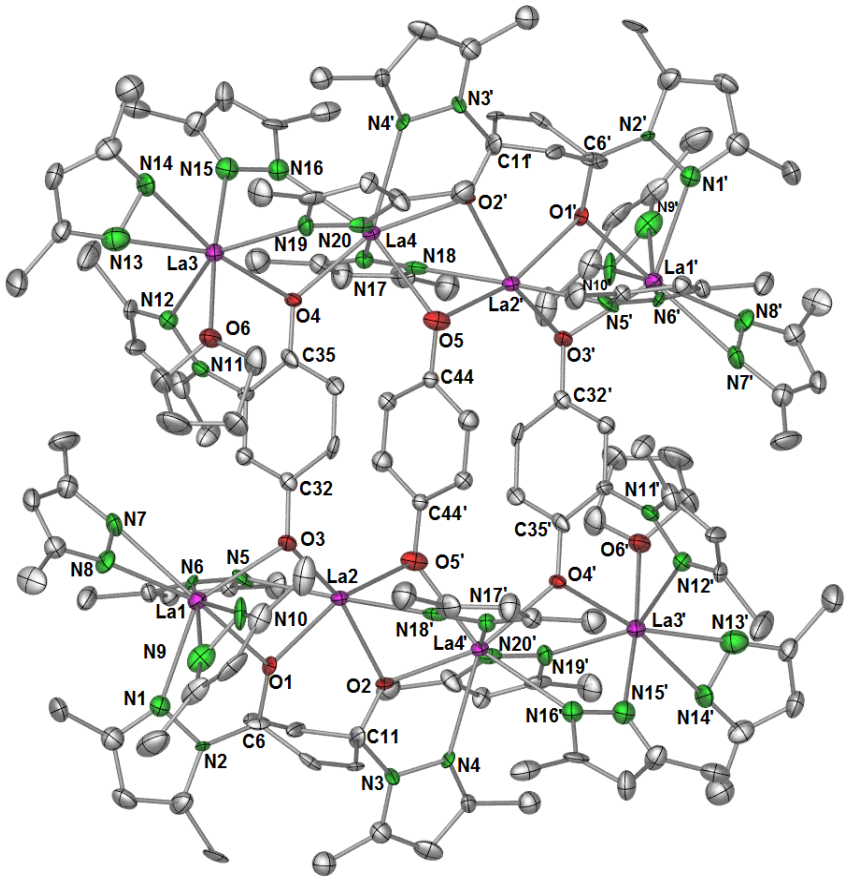

Table S7. Selected bond lengths of anionic ligands in [{$La_4(Me_2pz)_7$(pchd)(pzhq)(thf-d_8)}$_2$(hq)]·4PhMe (**4**)

Bond		Å	Bond		Å	Bond		Å
La1	O1	2.472(9)	La1	N1	2.611(13)	La2	N5	2.600(11)
La1	O3	2.480(9)	La1	N6	2.678(12)	La2	N18	2.584(12)
La2	O1	2.434(9)	La1	N7	2.548(14)	O5	C44	1.365(16)
La2	O2	2.481(10)	La1	N8	2.489(12)	La3	N12	2.621(11)
La2	O3	2.379(10)	La1	N9	2.453(13)	La3	N13	2.465(15)
La2	O5	2.441(10)	La1	N10	2.549(13)	La3	N14	2.489(14)
La3	O4	2.469(9)	O3	C32	1.392(17)	La3	N15	2.555(13)
La4	O4	2.407(9)	C6	O1	1.422(16)	La3	O6	2.559(10)
La4	O2′	2.402(10)	C6	N2	1.479(18)	La3	N19	2.543(12)
La4	O5′	2.495(10)	C11	O2	1.367(11)	C35	O4	1.347(17)

Bond		Å
La4	N16	2.594(12)
La4	N17	2.594(11)
La4	N20	2.657(11)
La4	N4′	2.661(12)